Online Appendix

Adaptation and the Mortality Effects of Temperature Across U.S. Climate Regions

Garth Heutel, Georgia State University and NBER
Nolan Miller, University of Illinois and NBER
David Molitor, University of Illinois and NBER

May 2020

Appendix A: Supplementary Material

A.1 Data Description

A.1.1 Medicare Data

Our baseline sample consists of Medicare beneficiaries age 65–100 and is derived from 100% Medicare enrollment information files for years 1992–2013.[1] These annual files include an observation for each beneficiary enrolled in Medicare for at least one day in that calendar year, whether enrolled in Original Medicare (fee-for-service) or Medicare Advantage. The enrollment files report a variety of demographic and enrollment variables, including unique beneficiary identifiers that link individuals over time; monthly indicators for Medicare eligibility; state, county, and ZIP code of residence based on the mailing address for official correspondence; and date of birth, date of death, and gender.

Medicare beneficiaries include the vast majority of elderly living in the United States. Appendix figure B.1a compares the number of Medicare beneficiaries in the enrollment files to census estimates of the number of U.S. resident population who are age 65 and over. To aid comparison, we use census estimates of the resident population on July 1 each year and limit the Medicare sample to beneficiaries residing in the 50 states and the District of Columbia and who turned 65 before July 1. Over the period 1992–2013, the census estimates an average of 36.7 million elderly individuals each year, compared to 35.9 million elderly beneficiaries in Medicare. Thus, the Medicare sample covers over 97% of elderly living in the United States, a share that remains roughly constant over the sample period.

The mortality variables used in our analysis are based on dates of death recorded in the Medicare enrollment files. Medicare's death data come primarily from the Social Security Administration but are augmented based on reviews triggered by hospitalization claims indicating patient death. The annual mortality rates in the Medicare data align closely to

[1] The Research Data Assistance Center (ResDAC) provides a helpful overview of the Medicare data files at http://www.resdac.org.

mortality rates based on National Vital Statistics death records and census population estimates, as shown in appendix figure B.1b. While all recorded deaths in the Medicare data are validated, some death *dates* in the data are not validated and are assigned the last date in the month of death. Because much of our analysis is performed at the daily level, we drop individuals who die at any point in the year and who do not have a validated death date flag. This restriction affects fewer than 3% of the deaths in our sample.

A.1.2 Daily Temperature and Climate Normals

GHCN-Daily Our primary source for daily temperature variables is the Global Historical Climatology Network (GHCN)-Daily database, which provides weather measurements from land surface stations across the United States, including the 48 adjoining U.S. states, the District of Columbia, Alaska, Hawaii, and Puerto Rico. We calculate daily high and low GHCN temperatures for each 2010 Census ZCTA as the inverse distance-weighted average of all available daily maximum and minimum temperatures, respectively, for GHCN stations within a 20-mile radius of the ZCTA centroid. The daily average GHCN temperature for a ZCTA is calculated as the midpoint of the daily high and low GHCN temperatures.

PRISM We also calculate daily temperature using the PRISM daily dataset. PRISM data provide interpolated daily temperature values at a 4km resolution and cover only the conterminous United States (the 48 adjoining U.S. states and the District of Columbia). We calculate daily high and low PRISM temperatures for each 2010 Census ZCTA as the inverse distance-weighted average of daily maximum and minimum temperatures, respectively, for PRISM grid points within a 20-mile radius of the ZCTA centroid. The daily average PRISM temperature for a ZCTA is calculated as the midpoint of the daily high and low PRISM temperatures.

Climate Normals We calculate climate summaries for each 2010 Census ZCTA using NOAA's 1980–2010 Climate Normals, which are produced for ground monitor stations across

the United States. ZCTA Climate Normals, for a given climate element, are calculated as the inverse distance-weighted average of Normals at the nearest station and any other stations within a 20-mile radius of the ZCTA centroid. The primary climate element we use in the analysis is CDD. For a given year, CDD is calculated as the (non-negative) number of degrees that a day's average temperature exceeds 65°F, summed over all days in a year. We also use average temperature Normals, which we calculate as the midpoint between the maximum and minimum temperature Normals.

A.1.3 Climate Models Data

We calculate end-of-century climate change predictions using all 21 climate models for which daily scenarios are produced and distributed as part of the Coupled Model Intercomparison Project Phase 5 (CMIP5). Daily downscaled projections for each of these models come from the NASA Earth Exchange Global Daily Downscaled Projections (NEX-GDDP) dataset. The NEX-GDDP data include daily minimum and maximum temperature predictions on a 25km by 25km grid (0.25-degree spatial resolution) for the period 1950–2100 (projections end in 2099 for some models). Projections for each model are made under two greenhouse gas emissions scenarios: the Representative Concentration Pathway (RCP) 8.5 "business as usual" scenario, where emissions continue to rise throughout the 21st century; and the RCP 4.5 scenario, a mid-range projection under which emissions peak around 2,040 and then decline.

For each of the 21 NEX-GDDP climate models, we construct grid-point-specific projected distributions of average daily temperature for both the current period (1992–2013) and the end-of-century period (2080–2099). To do so, we take the projected daily minimum and maximum temperatures over a given period, construct projected daily average temperature using the midpoint of daily maximum and minimum temperatures, and then calculate the fraction of days in which the projected daily average temperature falls into 1°F bins ranging from −30°F to 120°F.

To summarize the projected temperature distributions of the 21 NEX-GDDP climate models, we construct two "meta" models that average over each of the 21 component models as follows. First, for a given grid point, emissions scenario, and time period (current or end-of-century), we pool the daily projections of all 21 models. We calculate the unweighted distribution of these pooled daily projections and call this the "unweighted meta-distribution" of the "unweighted meta-model." We also compute the weighted distribution of pooled daily projections by weighting each daily projection by the model-specific weights employed by the Fourth National Climate Assessment that positively value model predictive skill but penalize codependency between models (Sanderson, Knutti and Caldwell, 2015; Sanderson and Wehner, 2017). We report these model weights in column 1 of appendix table B.2a. We call this weighted temperature distribution the "weighted meta-distribution" of the "weighted meta-model." Since the weighted meta-model is the primary model used in the paper, we also refer to these more concisely as the "meta-distribution" and the "meta-model."

A.2 Analysis Using PRISM Data

In this section, we present analogs to our main results where spatially interpolated temperature data from the PRISM Climate Group are used instead of the GHCN data. Although the PRISM data use a more sophisticated algorithm to assign temperatures to grid points (and then to ZIP codes), the algorithm it employs is less transparent than our simple distance weighting of the GHCN data. To the extent that the two methods differ, these differences tend to involve extreme temperatures, where the PRISM algorithm tends to assign less extreme values. In addition, while the GHCN data exist for the entire United States, including Alaska, Hawaii, and Puerto Rico, the PRISM data are limited to the contiguous United States. Because of the importance of extreme temperatures in our analysis and the fact that we do not know exactly why the PRISM algorithm moderates these days, we choose to use the distance-weighted data rather than the PRISM data. However, our results are qualitatively unchanged if PRISM data are used.

Appendix figure B.3 summarizes the distribution of realized temperature over the sample across each of 19 temperature bins ranging in 5°F increments from < 10°F to > 95°F. The gray-shaded region presents the distribution of daily average temperature for the United States as a whole, while line plots report the distribution separately for the coolest, middle, and warmest thirds of U.S. ZIP codes.

Appendix figure B.5 reproduces the main results of section 3 using PRISM weather data. Although the heterogeneous effects curves in the left panel are rotated slightly clockwise through the 60°F–65°F bin relative to the GHCN case (figure B.5a), the mortality results are qualitatively similar for both cases. The key reason for this is that, for both the GHCN and PRISM analyses, the homogeneous effects curve lies between the climate-specific effects curves for the warmest and coolest climate terciles, implying that using homogeneous effects will tend to overestimate the mortality impact of hot days in hot places and will underestimate their impact in cold places, with the opposite being true in the case of cold days. Numerical results corresponding to appendix figures B.5a and B.5b are presented in appendix tables B.1c and B.1d, respectively.

Appendix figure B.11 is a boxplot analogous to figure 5, using PRISM data instead of GHCN data. Although effect sizes are smaller, the same general patterns persist. In the homogeneous effects case (panel A), mortality effects increase as the regions get warmer, while in the heterogeneous effects case (panel B), mortality effects generally decrease as CDD increase. One exception is the coldest climates, where the effect of climate change is nearly zero. This could reflect that when PRISM data are used for estimating mortality effects, the implied mortality reduction from fewer very cold days is larger than when using GHCN data, which offsets much of the mortality increase from more very hot days.

Appendix table B.3 shows aggregate results for RCP 8.5 using PRISM data. Comparing it to the main results in table 1, which are based on GHCN data, the patterns are similar. Under homogeneous effects (column 5), the largest effects are once again found in the warmest third of ZIPs, while under heterogeneity with no adaptation (column 6), the effect on the

warmest third of ZIPs is much smaller than in the other two. While the mortality effect for the middle third of ZIP codes is larger under PRISM than GHCN, the standard error grows as well, suggesting that this increase may be driven by small changes in parts of the temperature distribution where mortality effects are large and imprecisely estimated (i.e., very hot days). All three terciles are expected to benefit from warming net of adaptation (column 7), although the coefficient is not statistically significant for the coolest third of ZIPs.

A.3 Analysis for the RCP 4.5 Emissions Scenario

As described in Van Vuuren et al. (2011), a Representative Concentration Pathway (RCP) is a comprehensive climate modeling scenario meant to capture possible climate change trajectories over the course of the century. The RCP 8.5 scenario we consider in our main analysis is a "business as usual" scenario where emissions continue to grow throughout the century. However, the climate models we consider also allow for consideration of the more moderate RCP 4.5 pathway, where emissions decline over the second half of the century and carbon dioxide concentrations stabilize around the year 2100.

The first four columns of table B.4 present summary statisics for the RCP 4.5 scenario for the United States overall and for each of the climate terciles. The RCP 4.5 scenario features more moderate warming, with an overall increase of 4.1°F, compared to the 8°F under RCP 8.5 reported in table 1. Each of the climate terciles also features an average temperature increase that is about half as large under RCP 4.5 as it is under RCP 8.5.

Figure B.10 presents a box plot for the RCP 4.5 scenario that can be compared to our main results for RCP 8.5 in figure 5. The qualitative patterns identified for the RCP 8.5 scenario persist in the RCP 4.5 scenario. Under homogeneous effects, the annual mortality change is increasing in CDD. As one might expect under a more modest warming scenario, the peak effect is about half as large as it is under RCP 8.5. The center and leftmost panels show each show effect sizes that decrease in CDD, again with generally smaller magnitudes

than under RCP 8.5.

Columns 5–7 of table B.4 present aggregate results for the RCP 4.5 scenario analogous to the corresponding results for RCP 8.5 reported in table 1. The main qualitative result—that the warmest third of ZIPs experiences the largest mortality impact under homogeneous effects (column 5) but in the smallest effect under heterogeneous effects (columns 6 and 7)—continues to hold for RCP 4.5, although the magnitudes are muted due to the smaller amount of overall warming embodied in RCP 4.5.

The mortality results for all U.S. ZIP codes are smaller under RCP 4.5 for the homogenous effects (0.18%) and heterogeneous effects with no adaptation (0.28%) cases than they were under RCP 8.5, again consistent with less overall warming. For the heterogeneous effects with adaptation case, the overall mortality effect is essentially zero (−0.06%) under RCP 4.5, whereas it was negative (−0.53%) under RCP 8.5. This could be driven by the fact that less adaptation takes place when there is less warming, as is the case under RCP 4.5.

A.4 Regional Heterogneity and Air Conditioning Adoption

There are two possible categories of explanations for regional heterogeneity in the temperature-mortality relationship. The first is that the heterogeneity is substantially due to changes in human physiology and behavior (i.e., adaptation). The second is that the regional differences we observe are due to characteristics that are correlated with current climate but not the results of human choices or physiology.

It is beyond the scope of this paper to identify each component of regional adaptation or to estimate how much regional heterogeneity is explained by each method of adaptation. However, in this section, we examine more closely one method of adaptation—residential AC—and the extent to which AC adoption can moderate the relationship between temperature and mortality. We find that differential AC adoption across climate regions is sufficient to explain their differences in mortality due to heat, but it cannot explain differential cold-related mortality. While we do not suggest that this should be interpreted as estimating the

causal effect of AC, it suggests that the temperature-mortality relationship can be moderated by currently available technologies such as AC adoption.

Because we do not observe AC adoption at the ZIP code level, we impute a value for the ZIP code penetration rate by fitting a machine learning (LASSO) model of AC adoption based on housing unit characteristics including housing stock age, geography, and climate and using data from the Residential Energy Consumption Survey (RECS), the American Community Survey (ACS), and the 2010 Census. This process requires constructing a set of comparable housing characteristics in both the RECS and census data.

A.4.1 Data Sources for Air Conditioning Imputation

We begin by describing the housing characteristics we use and how we define them in terms of original RECS and census variables.

Residential Energy Consumption Survey (RECS) Data. Our data on AC are derived from the RECS, which is administered by the Energy Information Administration (EIA) and surveys a nationally representative sample of housing units in the United States across 50 states and the District of Columbia. The RECS collects information on energy consumption and energy-related characteristics of housing units, including AC. We use RECS data from survey years 1993, 1997, 2001, 2005, and 2009. We model whether a housing unit in the RECS data has AC as a function of housing-level characteristics including the housing unit type, the geographic location of the housing unit, and the climate for the location of the unit. Below we describe the specific variables used in this model and how these variables are defined in terms of the original RECS variables from each year of the survey.

1. *Air conditioning (AC).* An indicator variable for whether a household reports to have AC equipment at home. This corresponds to the RECS variable AIRCOND ("Do you have air conditioning equipment at home") in years 1993, 1997, 2001, and 2005. For year 2009, the AIRCOND survey question changed to whether AC equipment is

"used." To obtain a consistent measure of AC ownership, for 2009, we instead rely on the variable DNTAC ("No air-conditioning equipment, or unused air-conditioning equipment"), which stratifies all households into three groups based on their report of AC ownership and usage status: (1) have AC equipment but do not use it, (2) have AC equipment and use it, and (3) do not have any AC equipment. We define a household unit to have AC equipment if it belongs to group (1) or (2).

2. *Year built.* A set of indicator variables (summing up to one for each household) identifying the decade when the housing unit was built (1939 or earlier, 1940 to 1949, ..., 1990 to 1999, 2000, or later). These variables are based on the RECS variable YEARMADE ("Year home built"), which reports the decadal interval when the home is built (mostly in early year) or the year the home is built. For each year, we group household units into decade built according to the categorization used by the 2007–2011 five-year ACS.

3. *Number of rooms.* A set of indicator variables (summing up to one for each household) identifying the number of rooms in the housing unit (one room, two rooms, ..., eight rooms, and nine or more rooms). For years 1993, 1997, and 2001, we count rooms by adding up RECS survey variables BEDROOMS ("Number of bedrooms") and OTHROOMS ("Number of other rooms"). We use the variable TOTROOMS ("Total number of rooms"), which is available for year 2005 and 2009. We then assign the number of rooms according to the categorization used by the 2007–2011 five-year ACS.

4. *Urban.* An indicator variable for whether the housing unit is in an urban area (i.e., nonrural area). This is based on the RECS variable UR (or URBRUR in early years). The RECS urban status information is obtained from interviewer observation (1993), household report (1997, 2001, 2005), and the Census Bureau's urban/rural geographic identifier (2009).

5. *Mobile.* An indicator variable for whether the housing unit is a mobile home. This

variable is based on the RECS variable TYPEHUQ ("Type of home as report by respondent"). TYPEHUQ reports whether the housing unit is mobile, single-family detached, single-family attached, apartment in a building with two to four units, or apartment in a building with more than five units.

6. *Own.* An indicator variable for whether the housing unit is owned. This is based on the RECS variable KOWNRENT ("Housing unit owned or rented"). KOWNRENT reports whether the housing unit is owned by someone in the household, rented, or occupied without payment.

7. *CDD65.* A continuous measure of cooling degree days (CDD) of the survey year with a base temperature of 65°F (i.e., the total number of degrees the daily temperature exceeds 65°F from January to December of the survey year). We draw this information from the RECS variable CDD65 (CD65 in earlier years). RECS creates this variable using temperature monitoring data from the National Climate Data Center's weather stations. A housing unit is first matched to the closest weather station, and then CDD is computed using the station's daily temperature data from January to December of the survey year. To mask the household location, a "random error" was added to the CDD. RECS does not provide further information regarding the structure of the random error.

8. *Census region.* A set of categorical variables (summing up to one for each household) identifying the census region location of the housing unit. This variable corresponds to the RECS variable REGIONC ("Census Region"), which includes Northeast, Midwest, South, and West Census Region.

9. *Census division.* A set of categorical variables (summing up to one for each household) identifying the census division location of the housing unit. This variable corresponds to the RECS variable DIVISION ("Census Division"). For years 1993, 1997, 2001, and 2005, DIVISION divides housing units into New England (CT, MA, ME, NH, RI,

VT), Middle Atlantic (NJ, NY, PA), East North Central (IL, IN, MI, OH, WI), West North Central (AR, LA, OK, TX), South Atlantic (DC, DE, FL, GA, MD, NC, SC, VA, WV), East South Central (AL, KY, MS, TN), West South Central (AR, LA, OK, TX), Mountain (AZ, CO, ID, MT, NM, NV, UT, WY), and Pacific Census Division (AK, CA, HI, OR, WA). In 2009, the Mountain Census Region is further divided into the Mountain North Sub-Division (CO, ID, MT, UT, WY) and the Mountain South Sub-Division (AZ, NM, NV). We combine the two groups to the single Mountain Division to keep the division identifier coherent across years.

10. *Sampling weights.* The sampling weight variable NWEIGHT provided by the RECS. This variable is the sampling weight for the observation in each survey year, which is equal approximately to the inverse of the probability of selection into the sample. RECS applies a couple of adjustments to the weights, including (1) adjustments to interview nonresponse, (2) post-stratification to match total energy consumption by fuel types, and (3) benchmarking to ensure that the total RECS weights add up to the ACS's total number of occupied housing units.

Census Data. We use ZIP-code-level housing characteristics from the 2007–2011 five-year ACS and the 2010 Census to construct a set of housing characteristics comparable to that which was used to predict AC using the LASSO model fit to the RECS data, described above. We obtain census data provided by the Minnesota Population Center (2016) through the National Historical Geographic Information System NHGIS16, and the variable names we refer to below are from the NHGIS.

1. *Year built.* Eight variables, each measuring the fraction of housing units that were built in 1939 or earlier, 1940 to 1949, ..., 1990 to 1999, and 2000 or later. We create these variables from the ACS variable "Year Structure Built," which counts total number of housing units built in each of the decadal intervals listed above. We convert counts to fractions by dividing the total number of housing units in the ZIP code.

2. *Number of rooms.* Nine variables, each measuring the fraction of housing units that have one room, two rooms, ..., eight rooms, and nine or more rooms. These variables are based on the ACS variable "Rooms." We convert counts to fractions by dividing the total number of housing units in the ZIP code.

3. *Urban.* Fraction of urban population from 2010 Census data. We divide the urban population in the ZIP code by the total population.

4. *Mobile.* Fraction of housing units that are mobile homes. We base this on the ACS variable "Units in Structure." which provides the number of mobile homes in the ZIP code, and we divide counts by the total number of housing units in the ZIP code.

5. *Own.* Fraction of occupied housing units that are owned. We draw this information from the ACS variable "Tenure by Household Size." We divide the number of owner-occupied housing units by the total number of occupied housing units in the ZIP code.

6. *CDD65.* Cooling degree days for the ZIP code, obtained from NOAA Climate Normals over the period 1980–2010 using inverse distance weighting of all monitors within a 20-mile radius of the ZIP code centroid.

7. *Census region.* A set of categorical variables (summing up to one for each ZIP code) identifying the census region of the ZIP code centroid. We use the U.S. Census Bureau's standard definition of census regions.

8. *Census division.* A set of categorical variables (summing up to one for each ZIP code) identifying the census division of the ZIP code centroid. We use the U.S. Census Bureau's standard definition of census divisions.

A.4.2 Air Conditioning Imputation Procedure

We use the housing characteristics from the RECS and 2010 Census described above to estimate a model of AC as a function of the location and characteristics of housing units.

Specifically, we estimate a housing-unit-level regression of whether the housing unit has AC equipment as a flexible function of CDD (a fourth-order polynomial) in the housing unit location, year built, number of rooms, urban location, mobile home status, and ownership status. We interact each of these housing characteristics with dummies for Census Region and Census Division. To avoid overfitting, we use LASSO penalized regression and select the penalty to minimize ten-fold cross-validated mean squared prediction error. We then apply this model to ZIP-code-level housing characteristics from the 2010 Census to compute predicted AC penetration for each U.S. ZIP code.

A potential cause of concern is that including local climate to predict local AC penetration could generate an artificial relationship between the mortality effects of temperature and AC adoption rates. While this could be an issue, empirically, AC adoption depends strongly on climate. As a result, omitting climate from the set of AC predictors introduces the possibility of systematic bias in the imputed AC measure that is correlated with climate. Because of this, our preferred imputation procedure includes local climate in the set of predictors. However, we also include results for an alternate imputation procedure that omits local climate variables.

A.4.3 Air Conditioning Results and Discussion

To estimate how temperature effects vary by AC penetration, we interact the imputed value of AC penetration (which is continuous between zero and one) with the temperature bins in equation 1. We also include in this regression Census Region by temperature bin fixed effects. Appendix figure B.12a, panel A, presents these regression results for three-day mortality outcomes. The curve represents the regression coefficients on the interaction between the AC penetration variable and the specified temperature bin. The interaction effects are significantly negative for temperatures above 70°F. For example, the coefficient on the interaction between AC penetration and the 80°F–85°F temperature bin is around −5, which implies that each 10 percentage point increase in AC penetration corresponds to 0.5 fewer

deaths per 100,000 individuals on an 80°F–85°F day. At hotter temperatures, the AC effect is even stronger: for example, the coefficient on the +95°F day bin implies about 1.8 fewer deaths per 100,000 for each 10 percentage point increase in AC penetration. By contrast, for temperatures below about 65°F, the interactions between AC and temperature tend to be quite small, indicating that the mortality effect of cold days is largely independent of the level of AC penetration.

Using these estimates as a linear estimate of the impact of AC adoption on mortality within each temperature bin, we calculate how much of the difference in heat sensitivity across regions can be explained by differences in AC penetration. Over the sample, AC penetration was 93.2% in the warmest ZIP codes, 82.1% in the middle third of ZIP codes, and 63.2% in the coolest. Panels B and C of appendix figure B.12a present counterfactual simulations, where we compute what the mortality curve would have been if the warmest ZIP codes had the AC penetration rates of the other two terciles, respectively. Thus, Panel B estimates what the temperature-mortality relationship would be in the warmest third of ZIP codes if the AC penetration rate in those ZIP codes were 30 percentage points lower than it actually is, as is the case in the coolest ZIP codes. The counterfactual warmest ZIP code curve closely tracks, and even rises, above the actual curve for the coolest ZIP codes at temperatures above 65°F–70°F, suggesting that differences in AC penetration can more than explain the differences in heat-related mortality between the warmest and coolest regions.[2]

At the same time, differences in AC penetration exacerbate the differences between the regions on cold days, consistent with AC as the mechanism driving the regional differences in heat-related mortality only. Panel C repeats this exercise, this time comparing a counterfactual where the warmest ZIP codes are adjusted for the approximately 11 percentage point difference in AC between the warmest and middle terciles. Once again, the counterfactual warmest tercile aligns closely with, but is slightly larger than, the middle tercile on hot days, again suggesting that differences in AC penetration account for a substantial portion of the

[2]If the impact of AC adoption on heat sensitivity is concave, that could explain why our projections using a linear estimate are too large.

estimated difference between the regions.[3]

These results extend the finding from Barreca et al. (2016) that increases in AC adoption over time can explain a substantial share of the reduction in heat-related mortality in the United States over the past century.[4] Our results show that in addition to explaining the reduction in heat-related mortality in the time-series, AC adoption can explain much of the cross-sectional differences in heat-related deaths observed across U.S. climate regions. These counterfactual exercises provide some support for the idea that the heterogeneity in temperature effects across climate regions we observe is driven by adaptation, and in particular AC, rather than by immutable regional characteristics. Thus, we might expect places to engage in this and other types of adaptive behavior in response to warming.

[3]Appendix figure B.12b reproduces the analysis using the alternative AC imputation procedure that excludes local climate variables. The results are very similar to those from the primary imputation procedure.

[4]Additionally, our results complement those of observational studies in the public health literature (e.g., Rogot, Sorlie and Backlund (1992)), which show that AC reduces the mortality impact of hot days.

Appendix B: Additional Figures and Tables

Figure B.1: Comparison of Medicare and Census Elderly Population and Mortality Rates

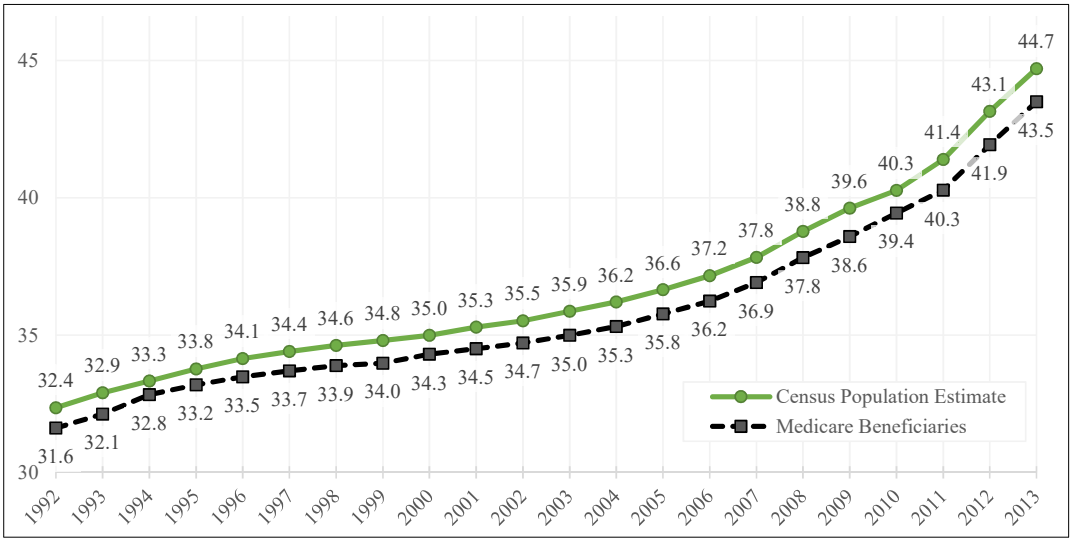

(a) Population (millions)

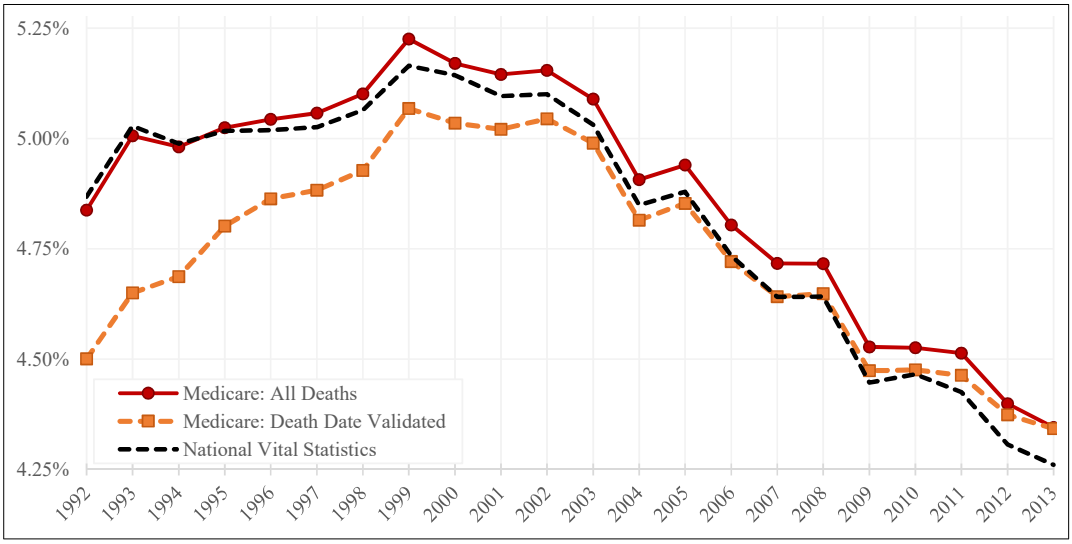

(b) Annual Mortality Rate

Panel (a): Census population estimates for the 50 United States and the District of Columbia come from the Compressed Mortality Files (CMF) 1979–1998 and 1999–2016. The population figures shown are April 1 Census counts in 2000 and 2010 and July 1 resident population estimates in other years. Medicare population counts include all beneficiaries in the annual Medicare enrollment file who were age 65 and over as of July 1 and had a U.S. ZIP code of residence in the 50 states or the District of Columbia.

Panel (b): National Vital Statistics mortality data come from the CMF described in Panel (a). National Vital Statistics mortality rates are calculated by dividing total CMF deaths among the 65 and over population in a given year by the Census population estimates shown in Panel (a). The dashed lines report annual mortality rates based on death dates recorded in the Medicare annual enrollment files. The figure reports both the total mortality rate in the Medicare sample ("Medicare: All Deaths"), as well as the mortality rate among the analytical sample used in the paper ("Medicare: Death Date Validated"), which excludes individuals who have a validated death that year but do not have a validated death *date* flag.

Figure B.2: U.S. Climate Normals: Cooling Degree Days

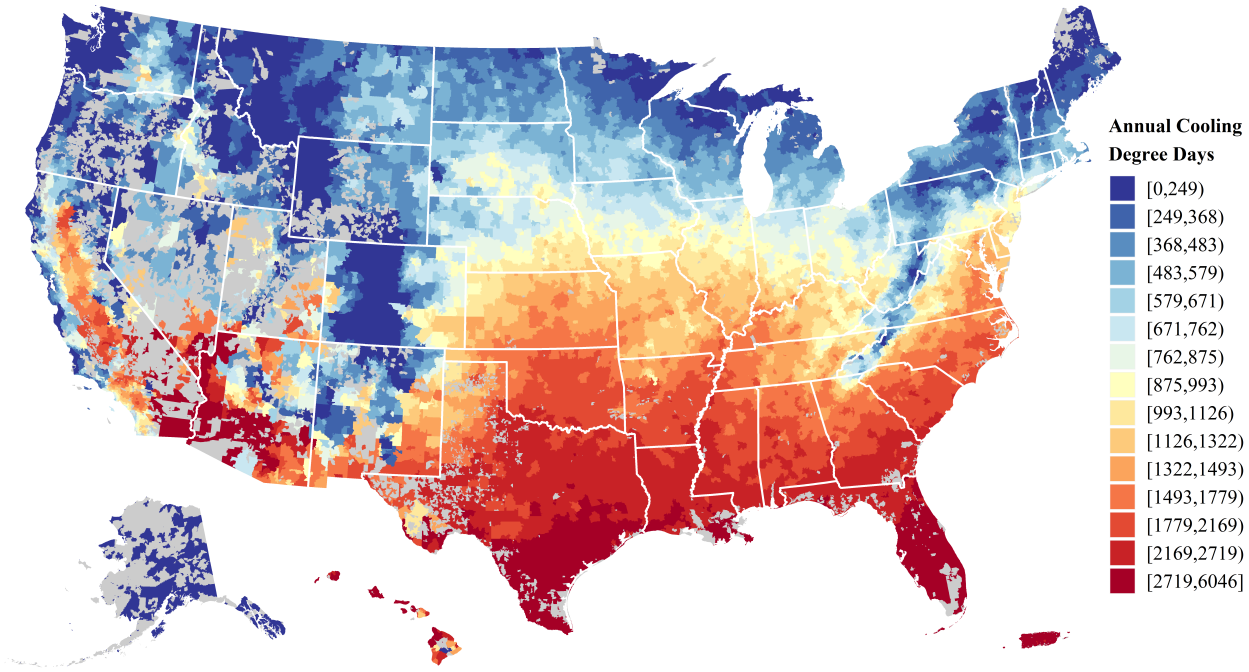

Notes: The figure shows the 1981–2010 cooling degree days (CDD) Climate Normals for the 2010 Census ZCTAs ($N = 33,120$). CDD Normals are available for 7,501 U.S. stations operated by the National Oceanic and Atmospheric Administration's National Weather Service. ZCTA Climate Normals are calculated as the inverse distance-weighted average of Normals at the nearest station and any other stations within a 20 mile radius of the ZCTA centroid. Gray regions represent parts of the U.S. that are not covered by a ZCTA.

Figure B.3: U.S. Daily Temperature Distribution (PRISM)

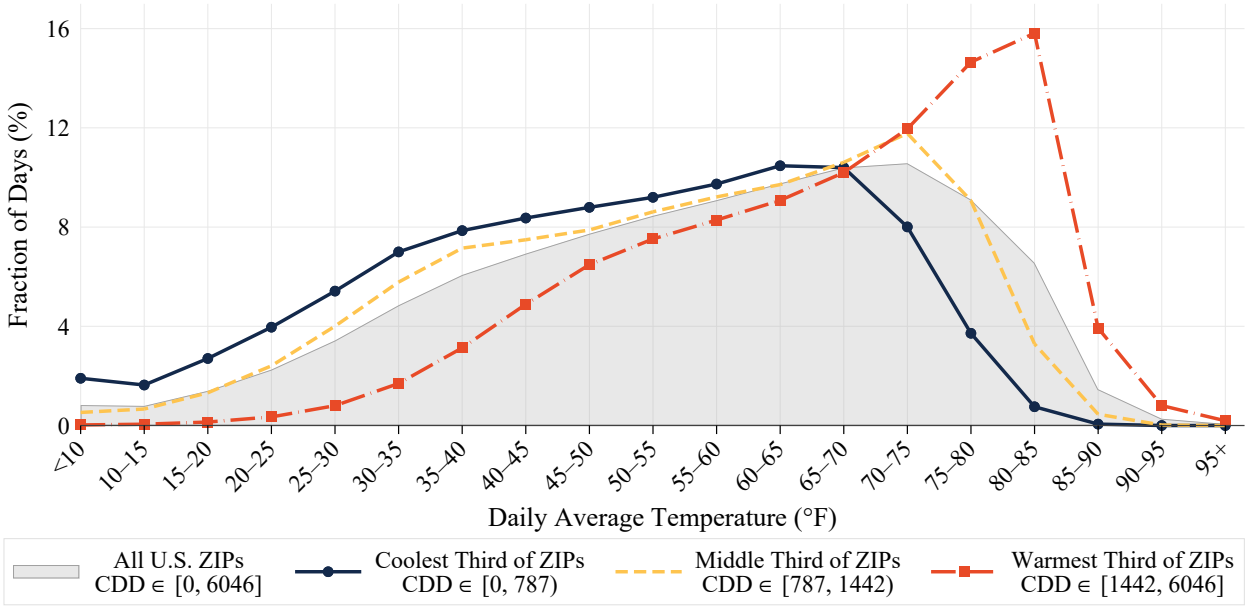

Notes: This figure summarizes the distribution of daily average temperature in the United States from 1992–2013. Distributions are reported separately for all U.S. ZIP codes and for the coolest, middle, and warmest population-weighted thirds of ZIP codes based on cooling degree days (CDD) Climate Normals. Daily temperature data come from the PRISM daily dataset and cover only the conterminous U.S. Appendix tables B.1c–B.1d report numerical values of the points in this figure. For comparison to daily temperature for the entire U.S. based on GHCN land station monitor data, see figure 1.

Figure B.4: Longer-Run Effects of Temperature on Mortality

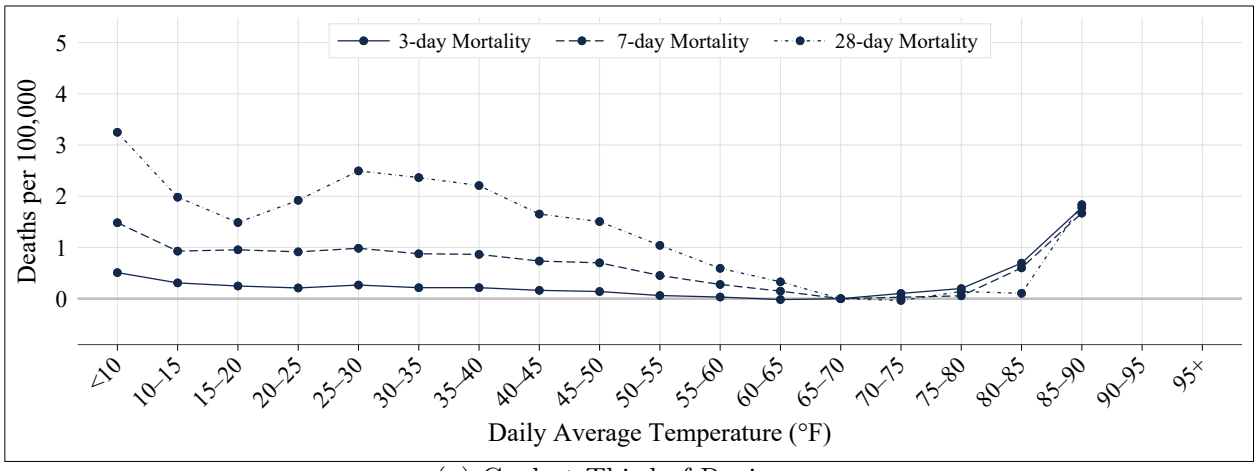

(a) Coolest Third of Regions

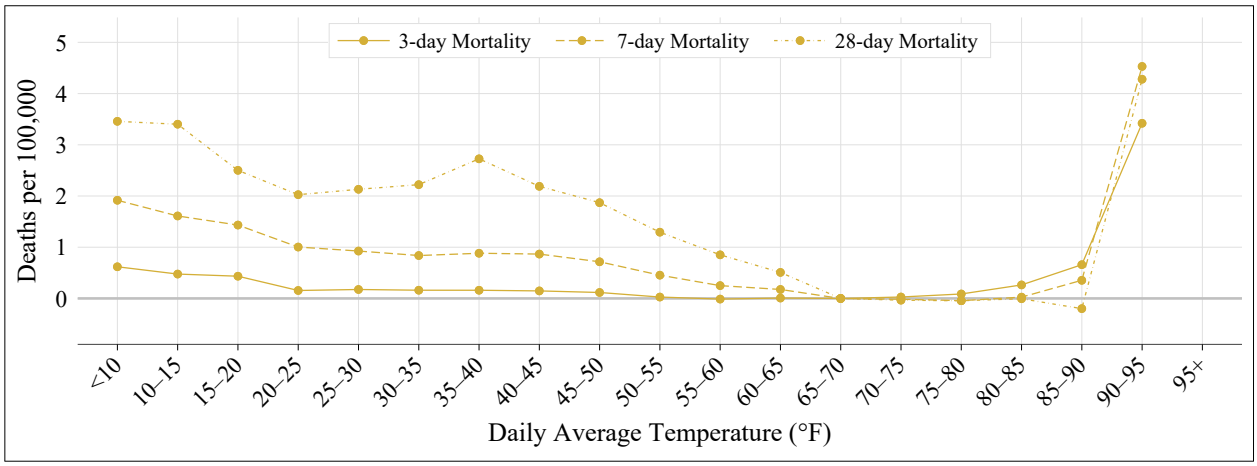

(b) Middle Third of Regions

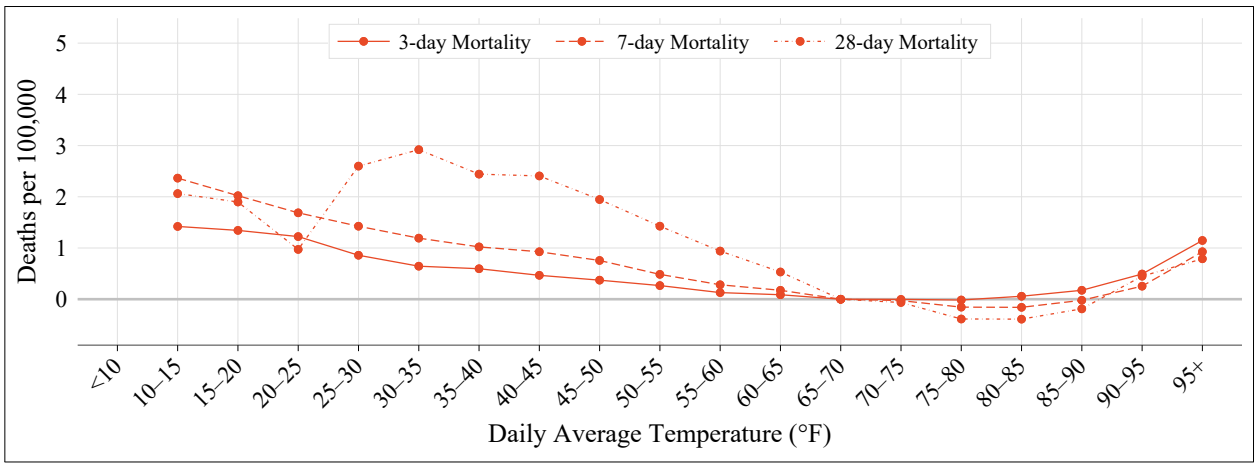

(c) Warmest Third of Regions

Notes: This figure presents coefficients from separate regressions for each of three outcome variables: 3-day, 7-day, and 28-day mortality. For all outcomes, the regression specification is that of Equation 1, but with temperature leads expanded to included average temperature in the 6 and 27 days following the event day.

Figure B.5: Effect of Temperature on Mortality (PRISM)

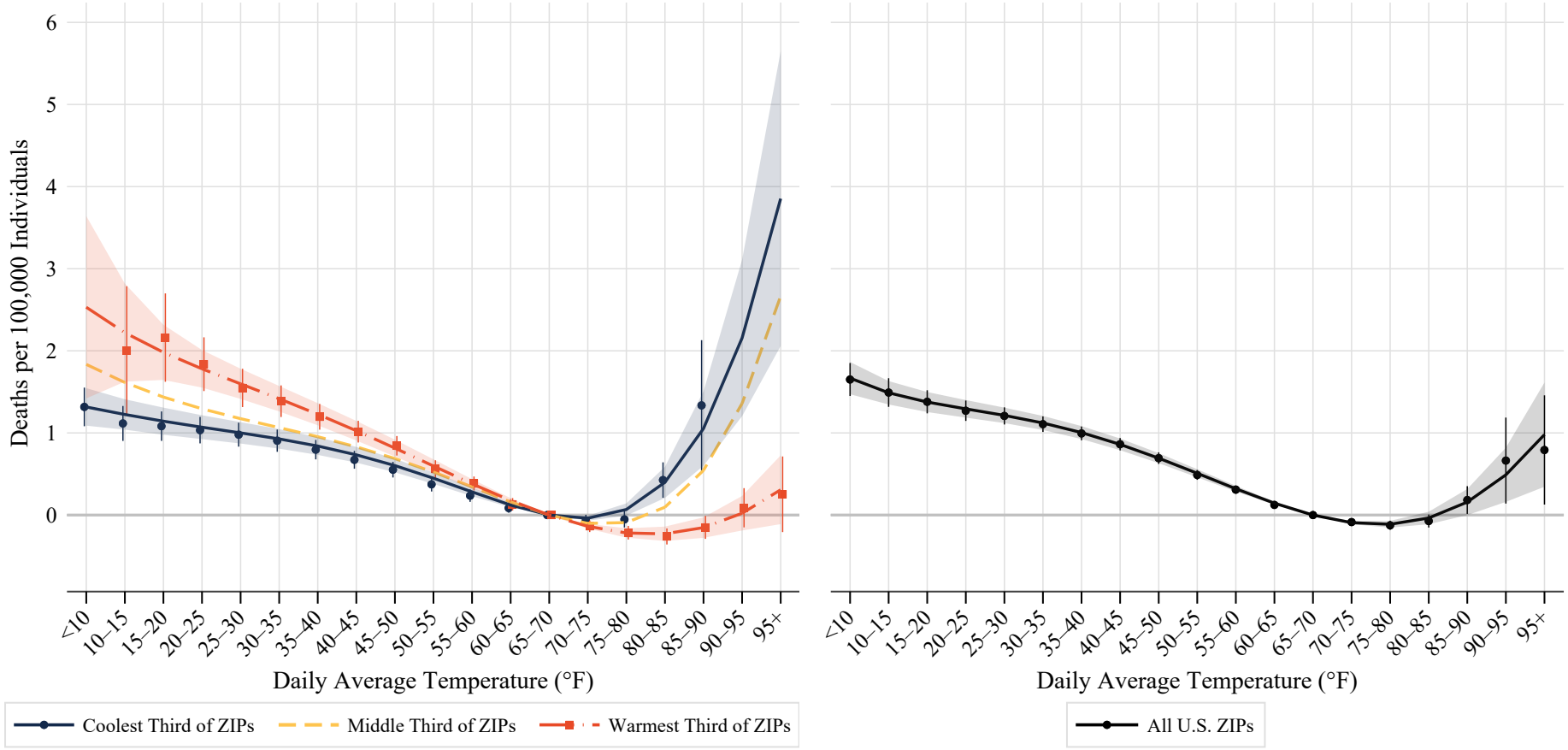

(a) Climate-Specific Temperature Effects

(b) Homogeneous Temperature Effects

Notes: This figure is analogous to figure 2 but plots estimated 3-day mortality effects of temperature as measured by PRISM data. In Panel (a), effects are allowed to differ by the coolest, middle, or warmest third of ZIP codes as defined in figure 1. In Panel (b), effects are restricted to be common to all U.S. ZIP codes. Effects reflect excess mortality on a day with a given average temperature relative to a day with an average temperature of 65°F–70°F. Markers with whisker lines plot non-parametric temperature bin estimates and associated 95 percent confidence intervals. Markers are only shown for binned temperatures that occur with a frequency of at least one day per decade in the climate region. Solid lines and shaded regions plot semi-parametric (5th degree polynomial in the temperature bins) estimates and associated 95 percent confidence intervals. Confidence intervals are based on two-way clustered standard errors at the county and state×date levels. Numerical values for all point estimates and standard errors are reported appendix tables B.1c–B.1d.

Figure B.6: Predicted Climate Change, 2080–2099 versus current

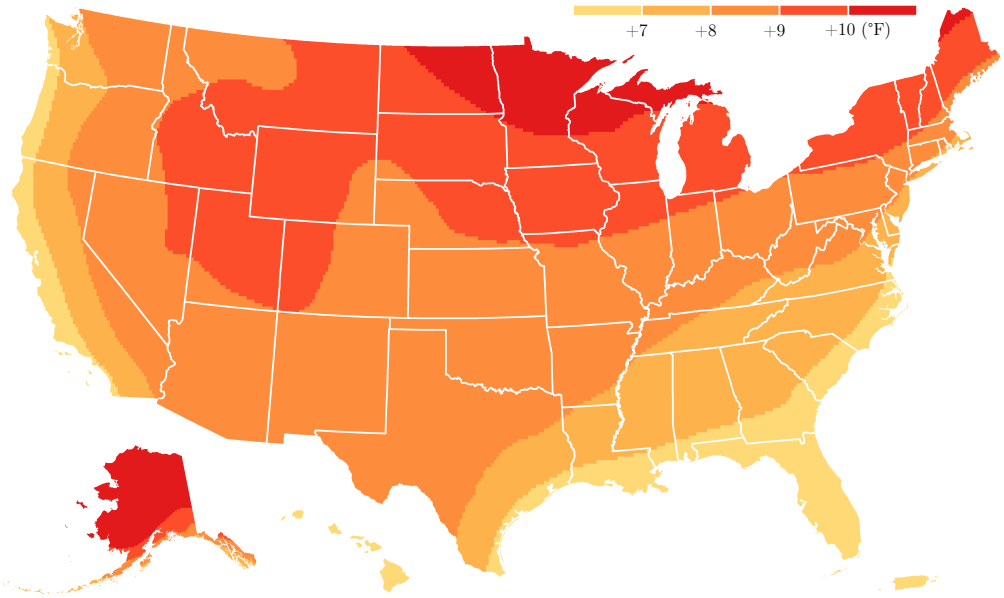

(a) Change in Average Temperature

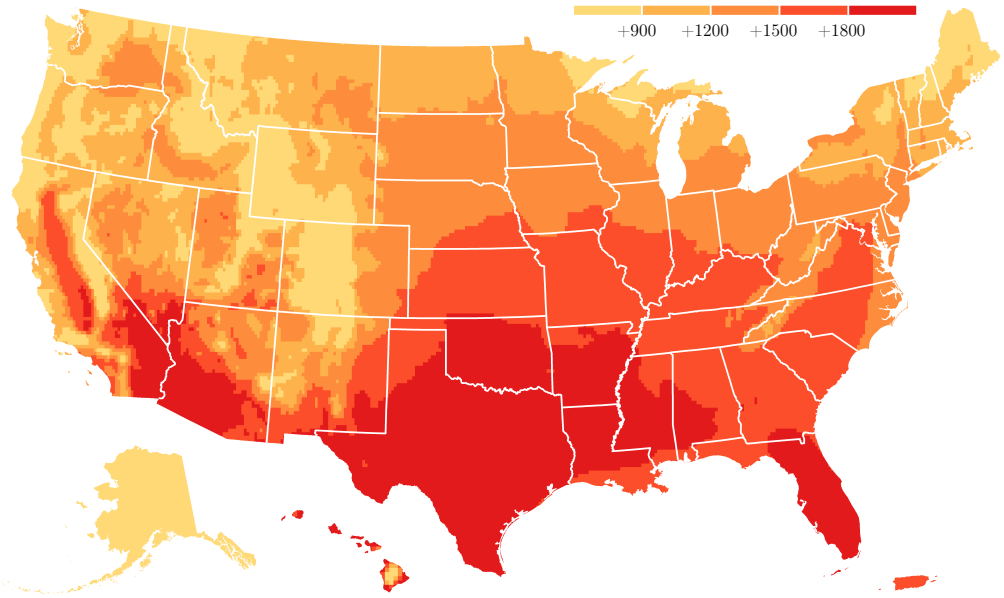

(b) Change in Annual Cooling Degree Days

Notes: The map shows projected end-of-century (2080–2099) changes in average temperature (panel (a)) and annual cooling degree days based on the meta-model,an average of the 21 NEX-GDDP climate models, under the RCP8.5emissions scenario. The map is shown at the resolution of the downscaled climate model output, which is produced on a 25km by 25km grid (0.25 degree spatial resolution).

Figure B.7: Parametric versus Nonparametric Effects of Temperature

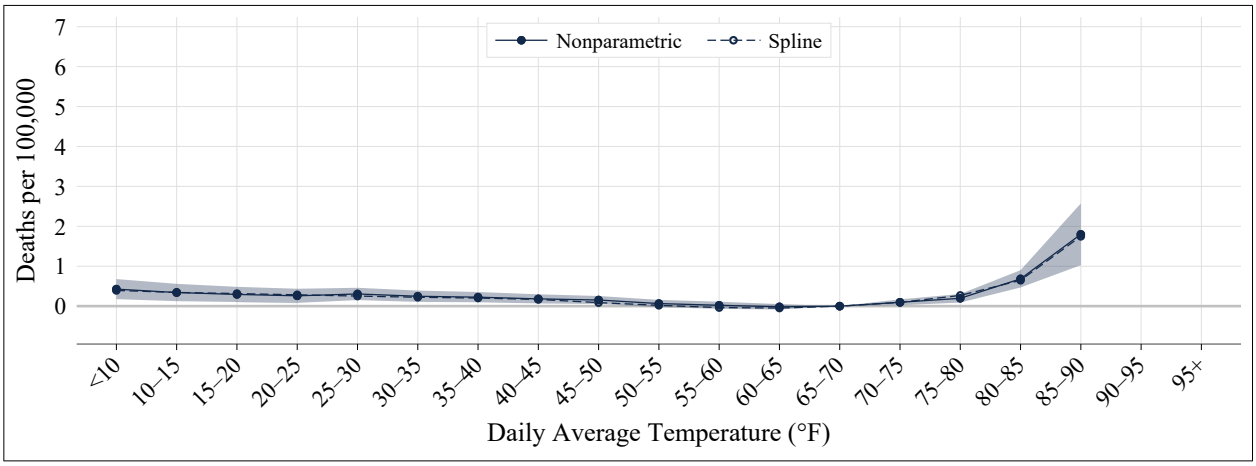

(a) Coolest Third of Regions

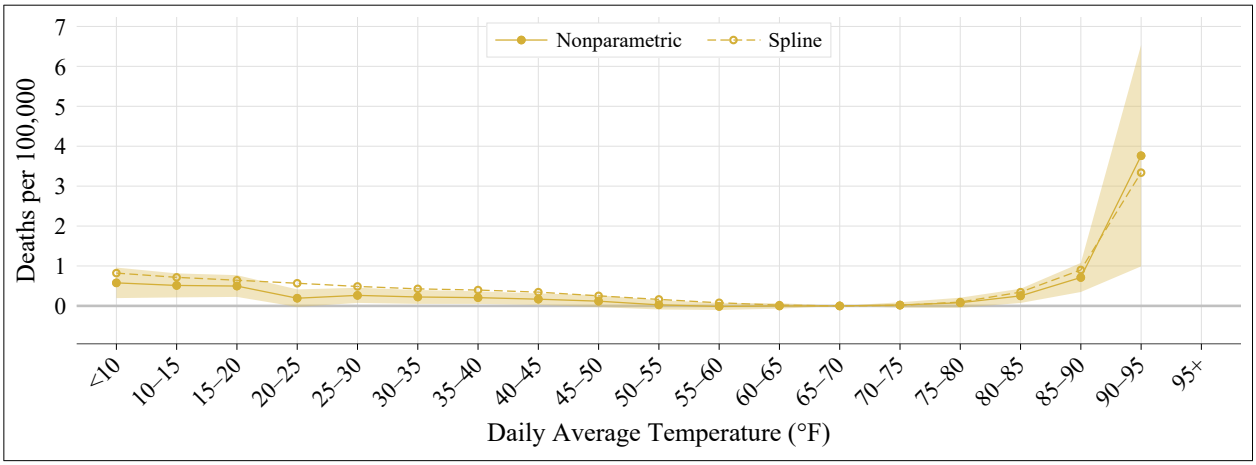

(b) Middle Third of Regions

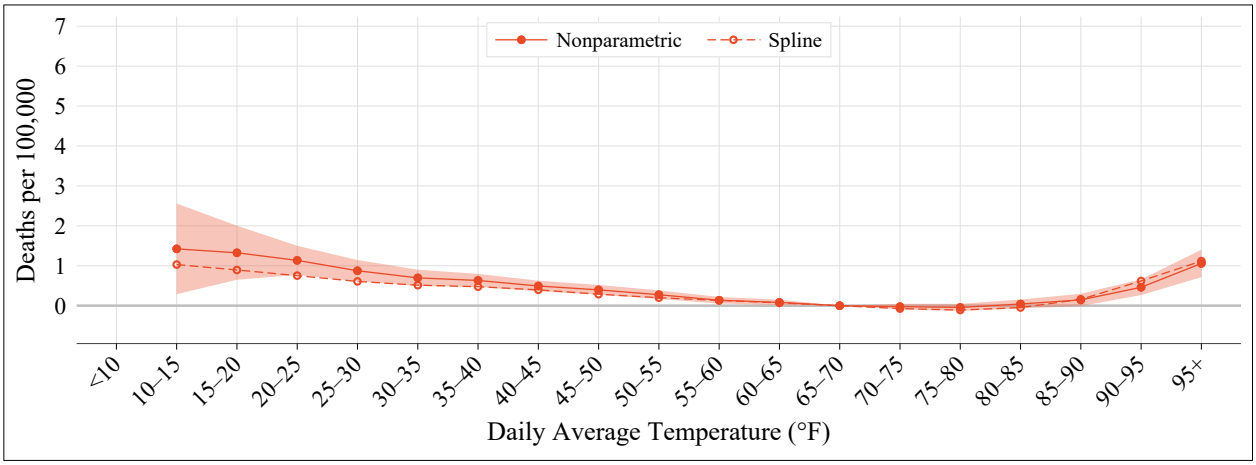

(c) Warmest Third of Regions

Notes: This figure summarizes how the estimated semi-parametric function of temperature and climate $f(t, CDD)$ performs relative to the nonparametric estimates of temperature effects by climate tercile reported in figure 2a. The "spline" estimates plotted with hollow markers come from re-estimating Equation (1) but with the fitted mortality values $\hat{f}(t, CDD)$ as the outcome and controlling only for temperature bin indicators. For comparison, the nonparametric estimates and corresponding 95 percent confidence intervals are plotted with solid markers and shaded area, respectively.

Figure B.8: Estimated Temperature Effects for Select ZIP Codes

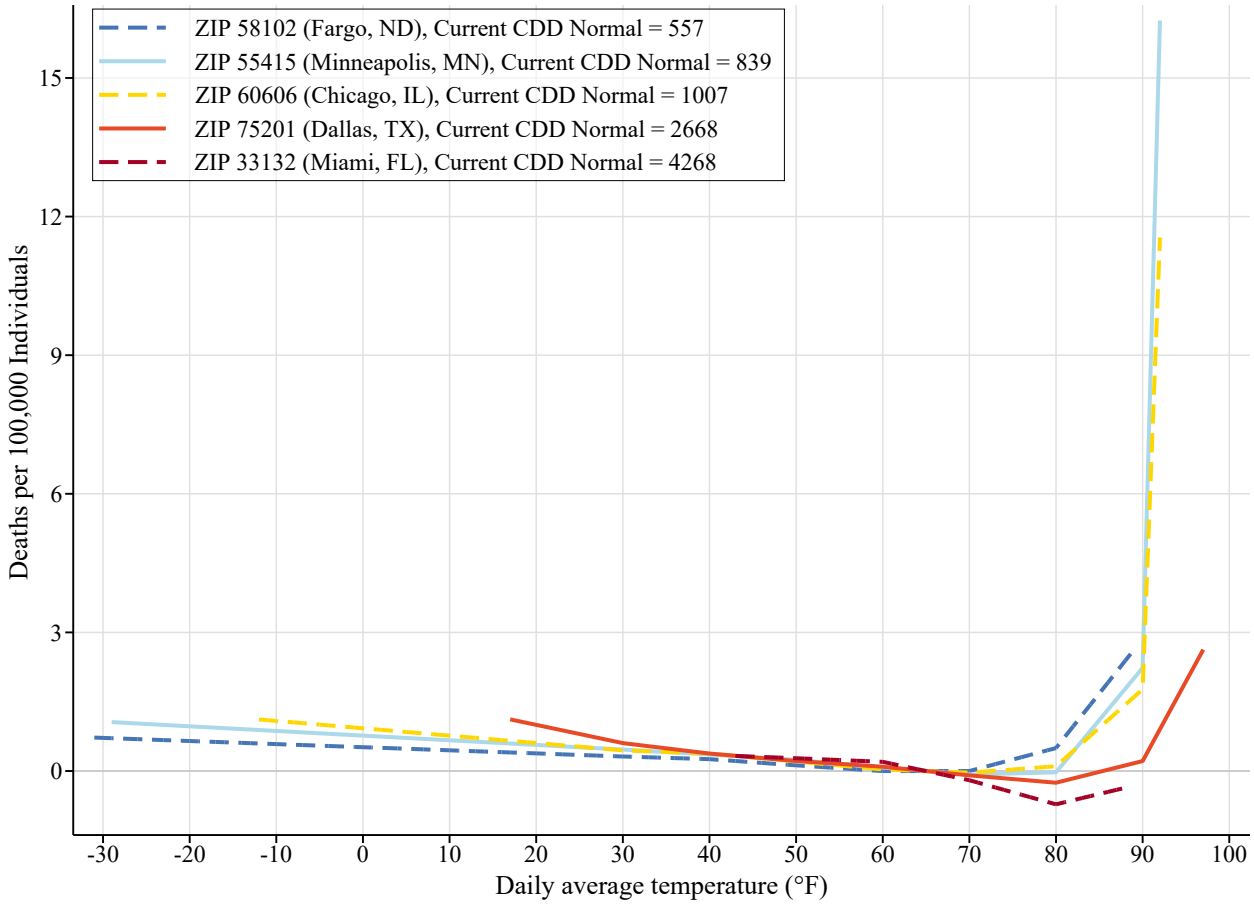

Notes: This figure illustrates estimates of the parametric spline $f(t, CDD)$ from Equation 3 by plotting the fitted temperature-mortality relationship for a selection of ZIP codes. For each ZIP code, $\hat{f}(t, CDD)$ is evaluated at the ZIP code's current CDD Normal and at all temperatures in the support of realized average daily temperatures for the ZIP code in the sample period 1992–2013.

Figure B.9a: Weighted Meta Model: End-of-Century Climate Change Effects (RCP 8.5)

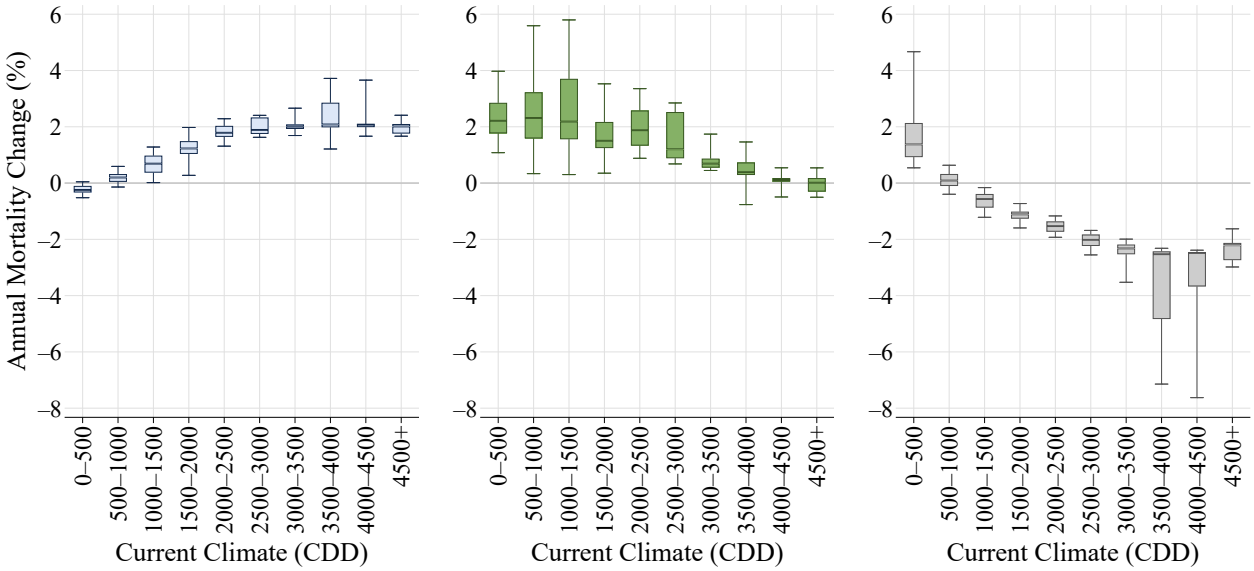

(a) Homogeneous Effects, No Adaptation

(b) Current Climate Effects, No Adaptation

(c) Current Climate Effects, Future Adaptation

Notes: The figure summarizes annual mortality effects of end-of-century (2080–2099) climate change relative to the current period (1992–2013) under the RCP 8.5 emissions scenario, as predicted by the weighted-meta-NEX-GDDP model. Observations are at the ZIP code level and are grouped by current climate (CDD). Box and whisker plots summarize the distribution of climate change effects across ZIP codes in each climate range. Boxes stretch from the 25th percentile (lower hinge) to the 75th percentile (upper hinge). The median is plotted as a line across the box. Whiskers stretch from the 5th percentile to the 95th percentile. Statistics are weighted by the elderly Medicare population in each ZIP code.

Figure B.9b: Unweighted Meta Model: End-of-Century Climate Change Effects (RCP 8.5)

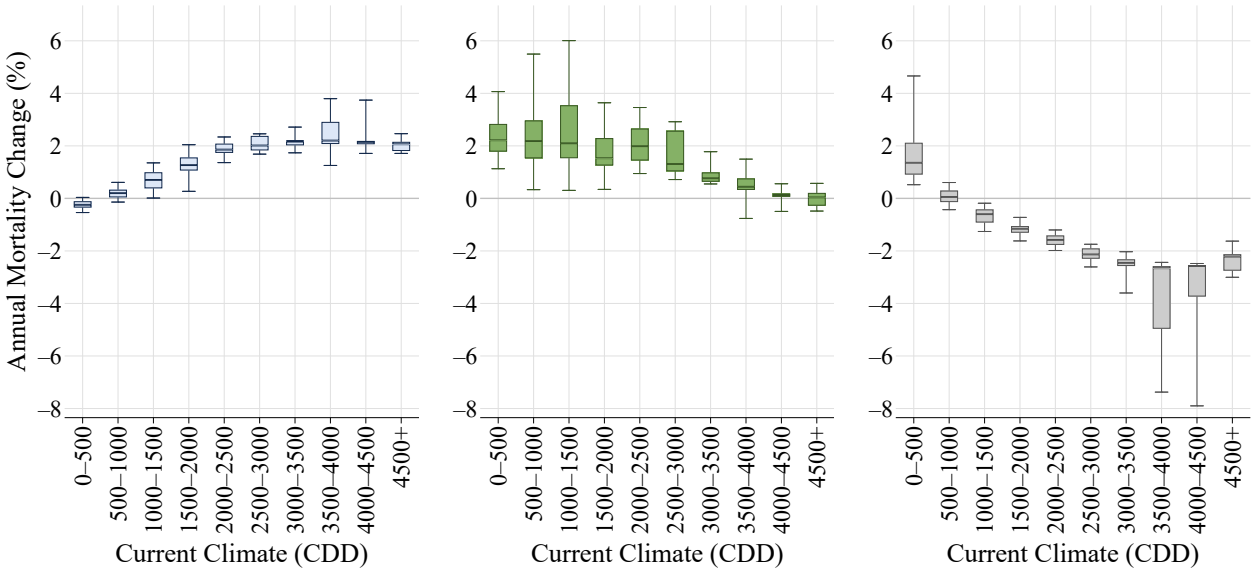

(a) Homogeneous Effects, No Adaptation

(b) Current Climate Effects, No Adaptation

(c) Current Climate Effects, Future Adaptation

Notes: The figure summarizes annual mortality effects of end-of-century (2080–2099) climate change relative to the current period (1992–2013) under the RCP 8.5 emissions scenario, as predicted by the meta-NEX-GDDP model. Box and whisker plots summarize ZIP code-level effects by current climate. Additional notes in Appendix Figure B.9a.

Figure B.9c: ACCESS1-0: End-of-Century Climate Change Effects (RCP 8.5)

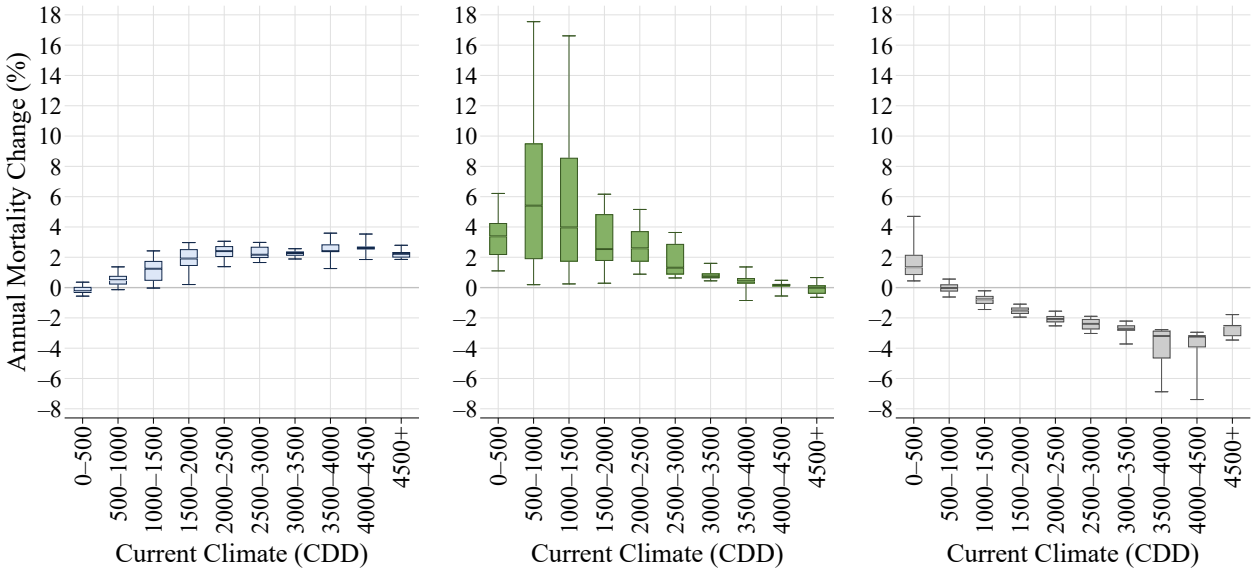

(a) Homogeneous Effects, No Adaptation

(b) Current Climate Effects, No Adaptation

(c) Current Climate Effects, Future Adaptation

Notes: The figure summarizes annual mortality effects of end-of-century (2080–2099) climate change relative to the current period (1992–2013) under the RCP 8.5 emissions scenario, as predicted by the ACCESS1-0 model. Box and whisker plots summarize ZIP code-level effects by current climate. Additional notes in Appendix Figure B.9a.

Figure B.9d: BNU-ESM: End-of-Century Climate Change Effects (RCP 8.5)

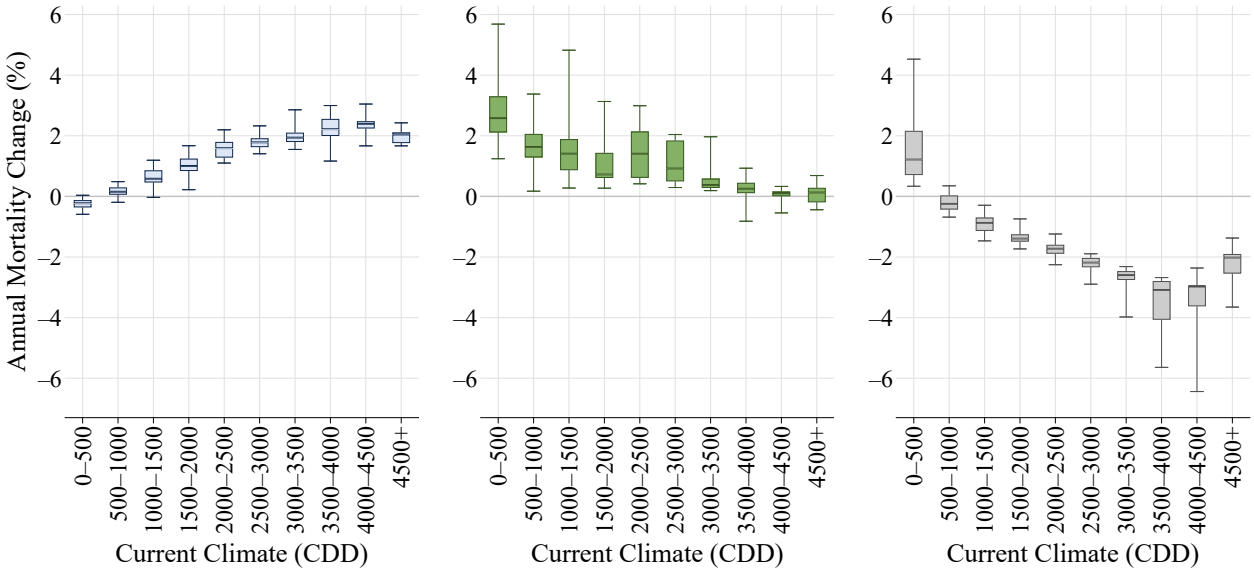

(a) Homogeneous Effects, No Adaptation

(b) Current Climate Effects, No Adaptation

(c) Current Climate Effects, Future Adaptation

Notes: The figure summarizes annual mortality effects of end-of-century (2080–2099) climate change relative to the current period (1992–2013) under the RCP 8.5 emissions scenario, as predicted by the BNU-ESM model. Box and whisker plots summarize ZIP code-level effects by current climate. Additional notes in Appendix Figure B.9a.

Figure B.9e: CCSM4: End-of-Century Climate Change Effects (RCP 8.5)

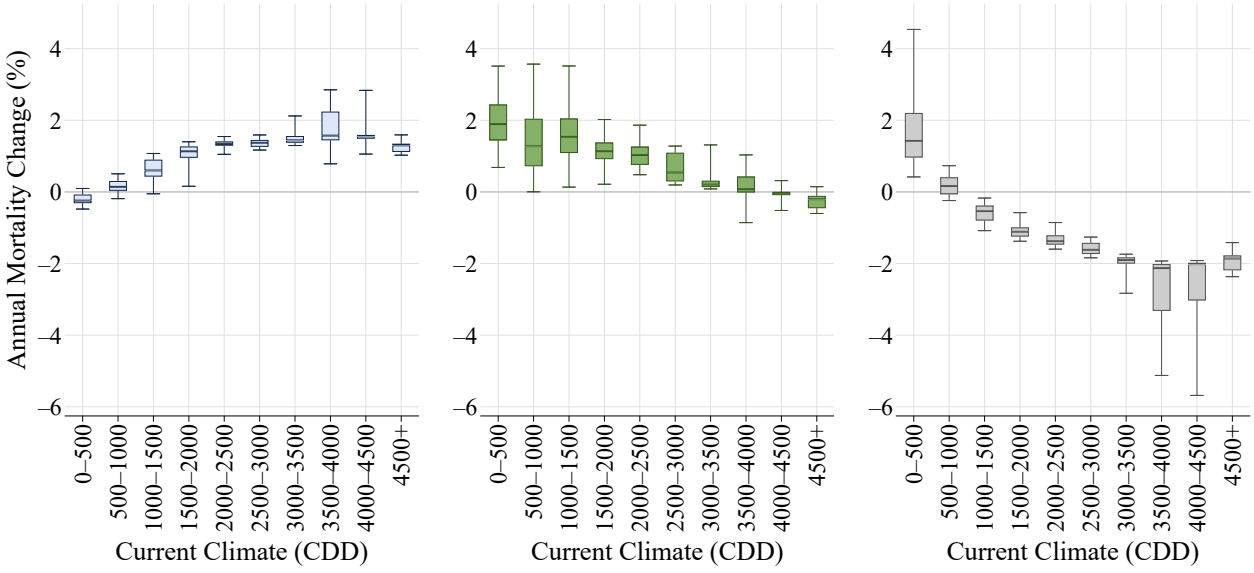

(a) Homogeneous Effects, No Adaptation

(b) Current Climate Effects, No Adaptation

(c) Current Climate Effects, Future Adaptation

Notes: The figure summarizes annual mortality effects of end-of-century (2080–2099) climate change relative to the current period (1992–2013) under the RCP 8.5 emissions scenario, as predicted by the CCSM4 model. Box and whisker plots summarize ZIP code-level effects by current climate. Additional notes in Appendix Figure B.9a.

Figure B.9f: CESM1-BGC: End-of-Century Climate Change Effects (RCP 8.5)

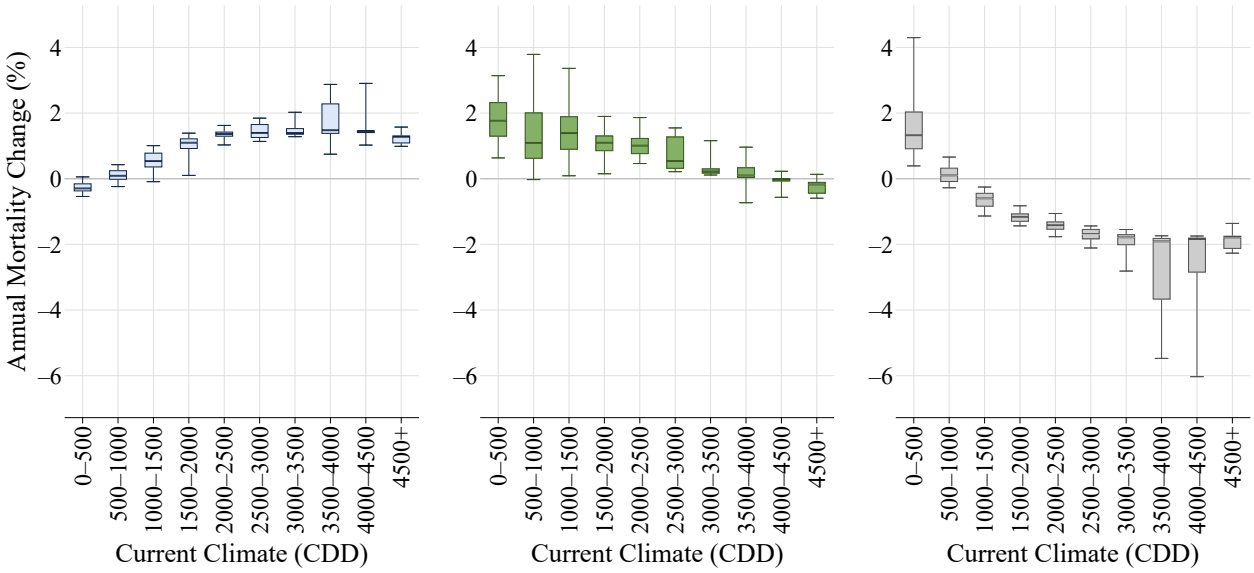

(a) Homogeneous Effects, No Adaptation

(b) Current Climate Effects, No Adaptation

(c) Current Climate Effects, Future Adaptation

Notes: The figure summarizes annual mortality effects of end-of-century (2080–2099) climate change relative to the current period (1992–2013) under the RCP 8.5 emissions scenario, as predicted by the CESM1-BGC model. Box and whisker plots summarize ZIP code-level effects by current climate. Additional notes in Appendix Figure B.9a.

Figure B.9g: CNRM-CM5: End-of-Century Climate Change Effects (RCP 8.5)

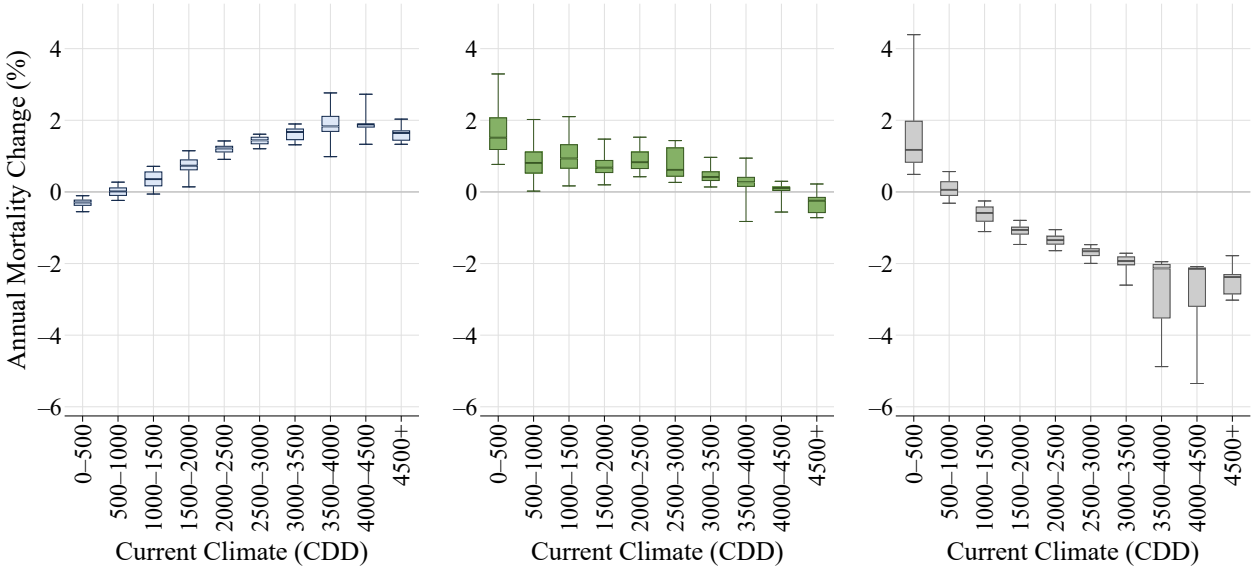

(a) Homogeneous Effects, No Adaptation

(b) Current Climate Effects, No Adaptation

(c) Current Climate Effects, Future Adaptation

Notes: The figure summarizes annual mortality effects of end-of-century (2080–2099) climate change relative to the current period (1992–2013) under the RCP 8.5 emissions scenario, as predicted by the CNRM-CM5 model. Box and whisker plots summarize ZIP code-level effects by current climate. Additional notes in Appendix Figure B.9a.

Figure B.9h: CSIRO-Mk3-6-0: End-of-Century Climate Change Effects (RCP 8.5)

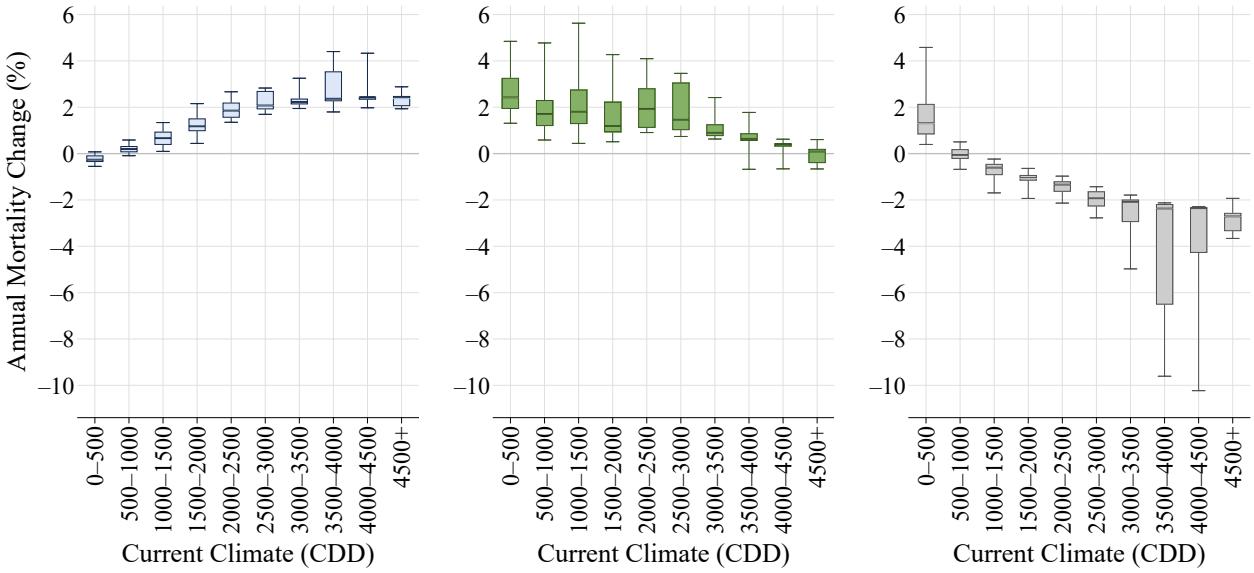

(a) Homogeneous Effects, No Adaptation

(b) Current Climate Effects, No Adaptation

(c) Current Climate Effects, Future Adaptation

Notes: The figure summarizes annual mortality effects of end-of-century (2080–2099) climate change relative to the current period (1992–2013) under the RCP 8.5 emissions scenario, as predicted by the CSIRO-Mk3-6-0 model. Box and whisker plots summarize ZIP code-level effects by current climate. Additional notes in Appendix Figure B.9a.

Figure B.9i: CanESM2: End-of-Century Climate Change Effects (RCP 8.5)

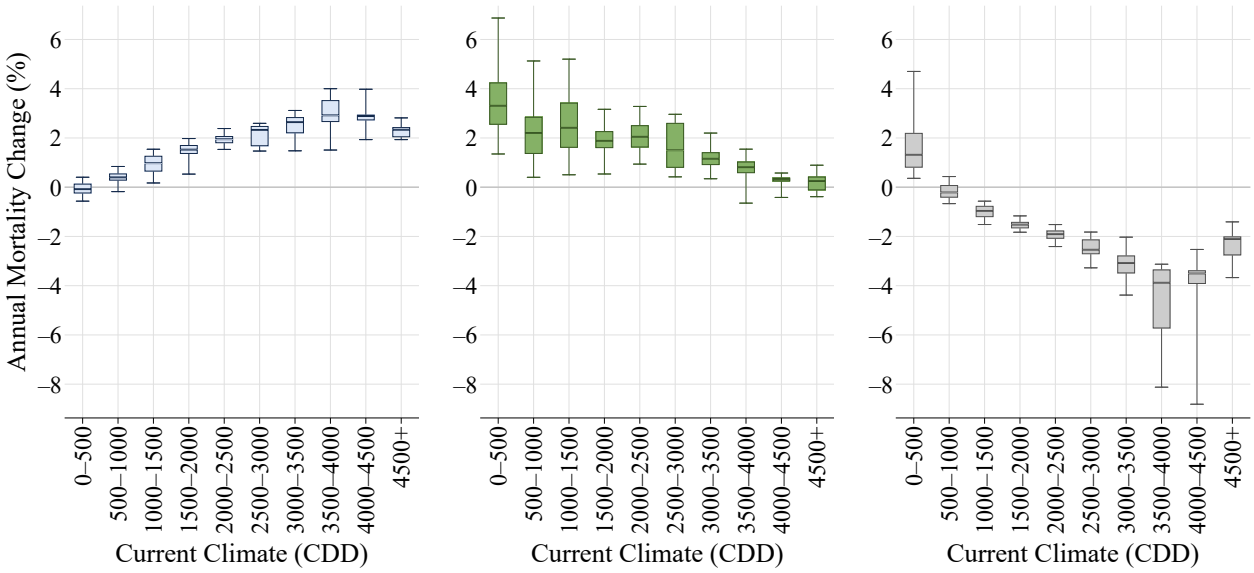

(a) Homogeneous Effects, No Adaptation

(b) Current Climate Effects, No Adaptation

(c) Current Climate Effects, Future Adaptation

Notes: The figure summarizes annual mortality effects of end-of-century (2080–2099) climate change relative to the current period (1992–2013) under the RCP 8.5 emissions scenario, as predicted by the CanESM2 model. Box and whisker plots summarize ZIP code-level effects by current climate. Additional notes in Appendix Figure B.9a.

Figure B.9j: GFDL-CM3: End-of-Century Climate Change Effects (RCP 8.5)

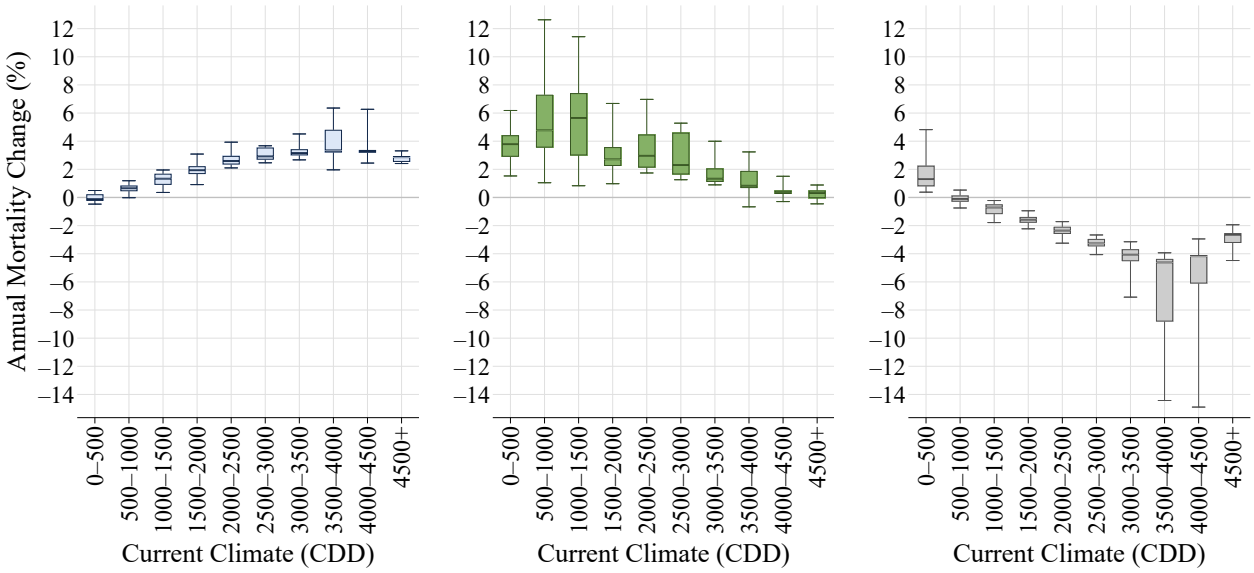

(a) Homogeneous Effects, No Adaptation

(b) Current Climate Effects, No Adaptation

(c) Current Climate Effects, Future Adaptation

Notes: The figure summarizes annual mortality effects of end-of-century (2080–2099) climate change relative to the current period (1992–2013) under the RCP 8.5 emissions scenario, as predicted by the GFDL-CM3 model. Box and whisker plots summarize ZIP code-level effects by current climate. Additional notes in Appendix Figure B.9a.

Figure B.9k: GFDL-ESM2G: End-of-Century Climate Change Effects (RCP 8.5)

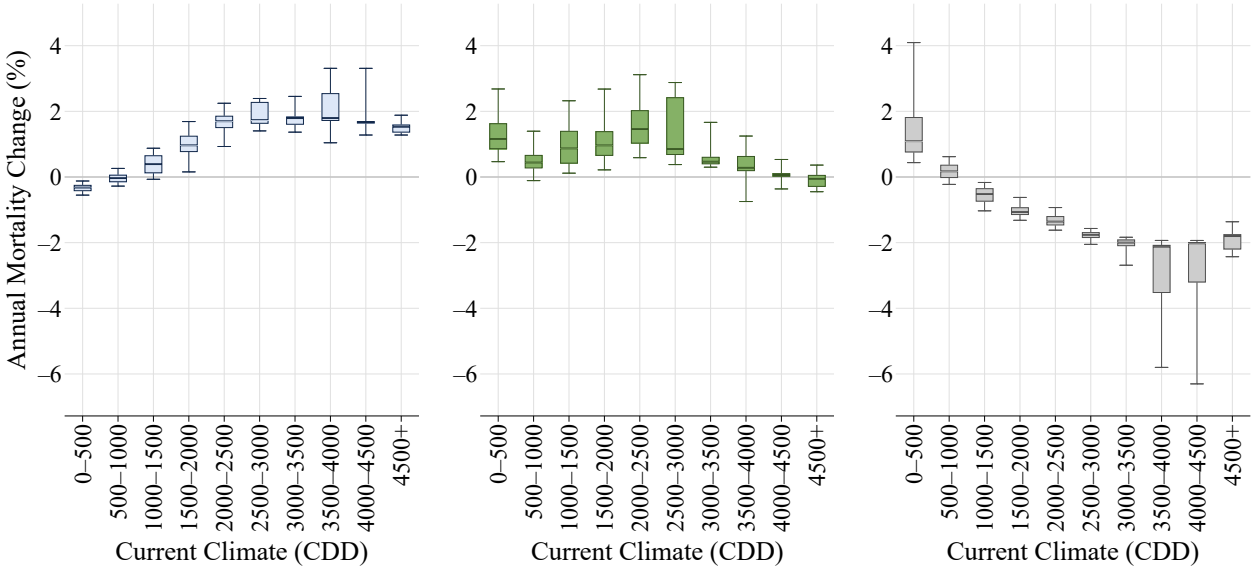

(a) Homogeneous Effects, No Adaptation

(b) Current Climate Effects, No Adaptation

(c) Current Climate Effects, Future Adaptation

Notes: The figure summarizes annual mortality effects of end-of-century (2080–2099) climate change relative to the current period (1992–2013) under the RCP 8.5 emissions scenario, as predicted by the GFDL-ESM2G model. Box and whisker plots summarize ZIP code-level effects by current climate. Additional notes in Appendix Figure B.9a.

Figure B.9l: GFDL-ESM2M: End-of-Century Climate Change Effects (RCP 8.5)

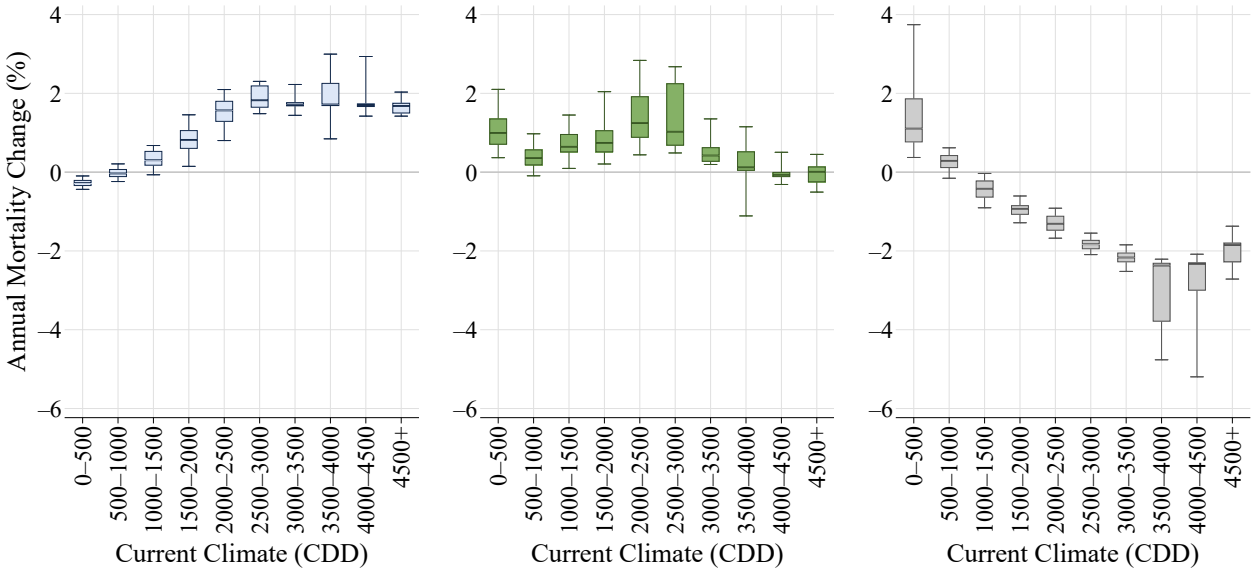

(a) Homogeneous Effects, No Adaptation

(b) Current Climate Effects, No Adaptation

(c) Current Climate Effects, Future Adaptation

Notes: The figure summarizes annual mortality effects of end-of-century (2080–2099) climate change relative to the current period (1992–2013) under the RCP 8.5 emissions scenario, as predicted by the GFDL-ESM2M model. Box and whisker plots summarize ZIP code-level effects by current climate. Additional notes in Appendix Figure B.9a.

Figure B.9m: IPSL-CM5A-LR: End-of-Century Climate Change Effects (RCP 8.5)

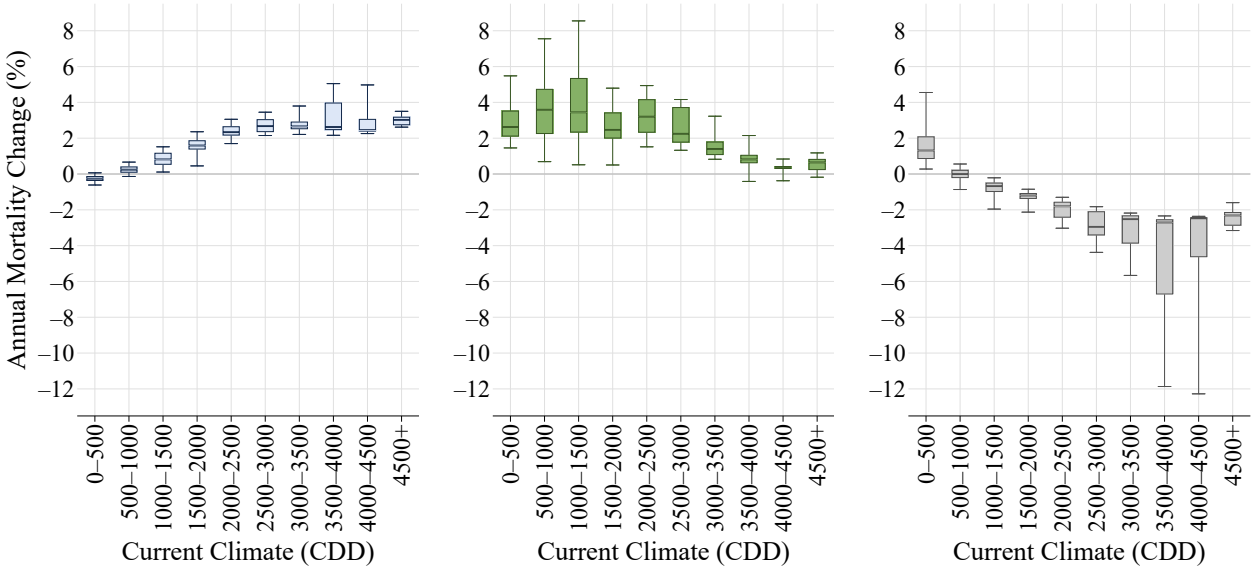

(a) Homogeneous Effects, No Adaptation

(b) Current Climate Effects, No Adaptation

(c) Current Climate Effects, Future Adaptation

Notes: The figure summarizes annual mortality effects of end-of-century (2080–2099) climate change relative to the current period (1992–2013) under the RCP 8.5 emissions scenario, as predicted by the IPSL-CM5A-LR model. Box and whisker plots summarize ZIP code-level effects by current climate. Additional notes in Appendix Figure B.9a.

Figure B.9n: IPSL-CM5A-MR: End-of-Century Climate Change Effects (RCP 8.5)

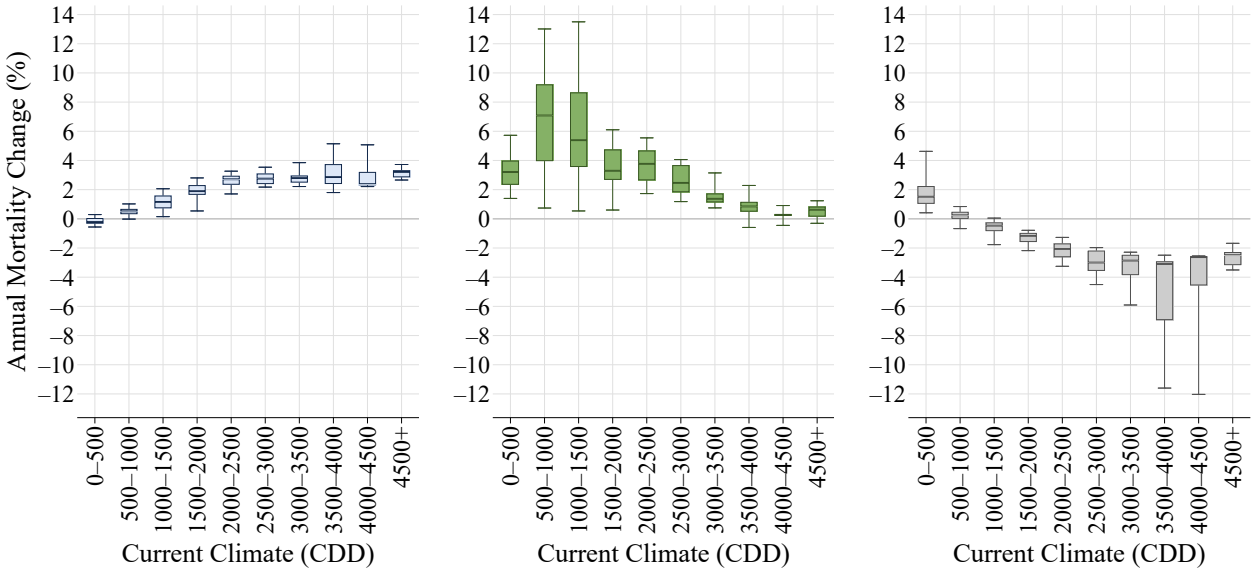

(a) Homogeneous Effects, No Adaptation

(b) Current Climate Effects, No Adaptation

(c) Current Climate Effects, Future Adaptation

Notes: The figure summarizes annual mortality effects of end-of-century (2080–2099) climate change relative to the current period (1992–2013) under the RCP 8.5 emissions scenario, as predicted by the IPSL-CM5A-MR model. Box and whisker plots summarize ZIP code-level effects by current climate. Additional notes in Appendix Figure B.9a.

Figure B.9o: MIROC-ESM: End-of-Century Climate Change Effects (RCP 8.5)

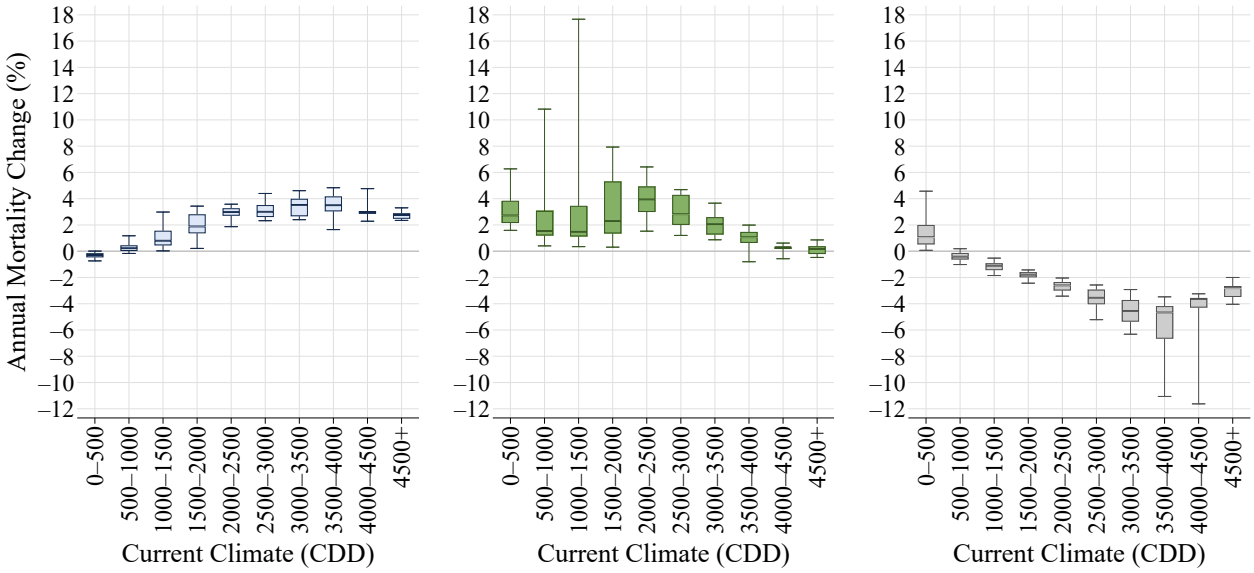

(a) Homogeneous Effects, No Adaptation

(b) Current Climate Effects, No Adaptation

(c) Current Climate Effects, Future Adaptation

Notes: The figure summarizes annual mortality effects of end-of-century (2080–2099) climate change relative to the current period (1992–2013) under the RCP 8.5 emissions scenario, as predicted by the MIROC-ESM model. Box and whisker plots summarize ZIP code-level effects by current climate. Additional notes in Appendix Figure B.9a.

Figure B.9p: MIROC-ESM-CHEM: End-of-Century Climate Change Effects (RCP 8.5)

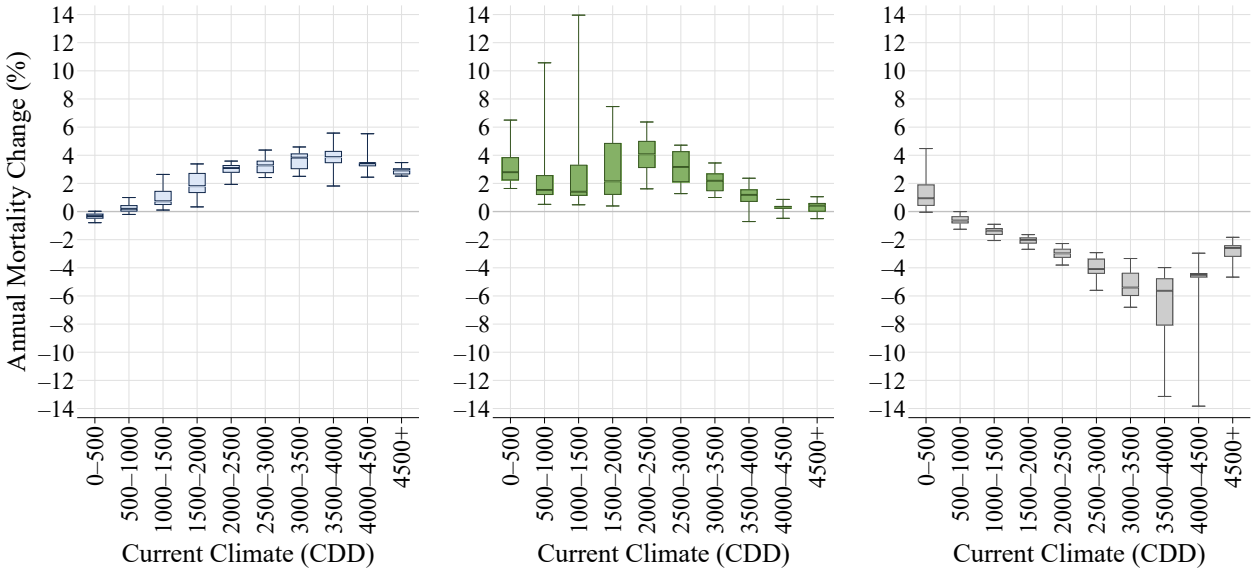

(a) Homogeneous Effects, No Adaptation

(b) Current Climate Effects, No Adaptation

(c) Current Climate Effects, Future Adaptation

Notes: The figure summarizes annual mortality effects of end-of-century (2080–2099) climate change relative to the current period (1992–2013) under the RCP 8.5 emissions scenario, as predicted by the MIROC-ESM-CHEM model. Box and whisker plots summarize ZIP code-level effects by current climate. Additional notes in Appendix Figure B.9a.

Figure B.9q: MIROC5: End-of-Century Climate Change Effects (RCP 8.5)

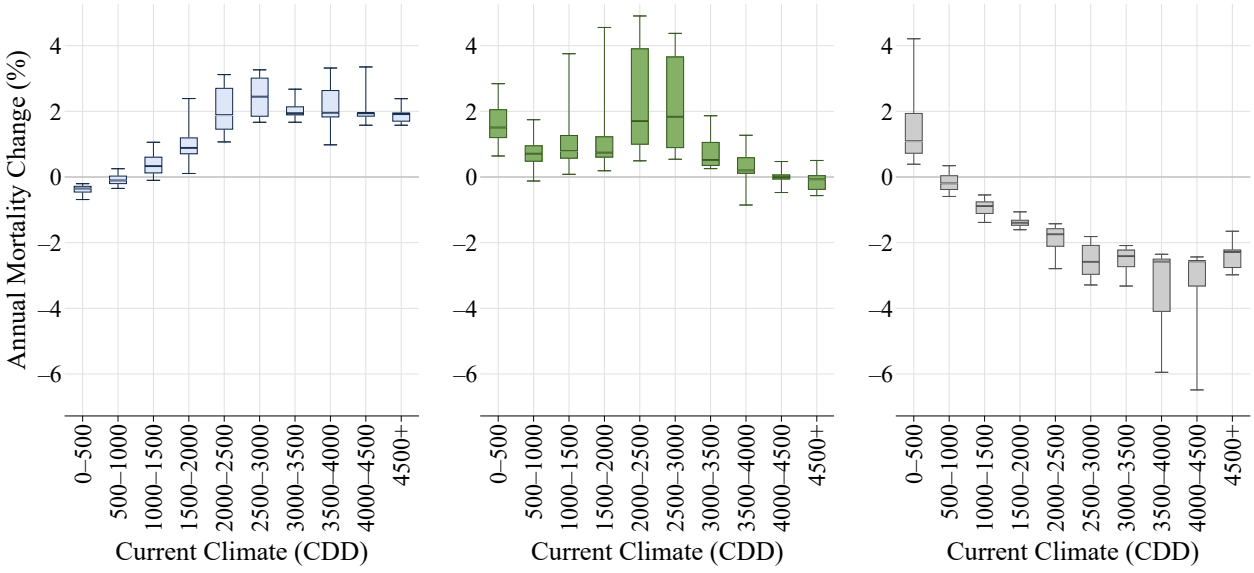

(a) Homogeneous Effects, No Adaptation

(b) Current Climate Effects, No Adaptation

(c) Current Climate Effects, Future Adaptation

Notes: The figure summarizes annual mortality effects of end-of-century (2080–2099) climate change relative to the current period (1992–2013) under the RCP 8.5 emissions scenario, as predicted by the MIROC5 model. Box and whisker plots summarize ZIP code-level effects by current climate. Additional notes in Appendix Figure B.9a.

Figure B.9r: MPI-ESM-LR: End-of-Century Climate Change Effects (RCP 8.5)

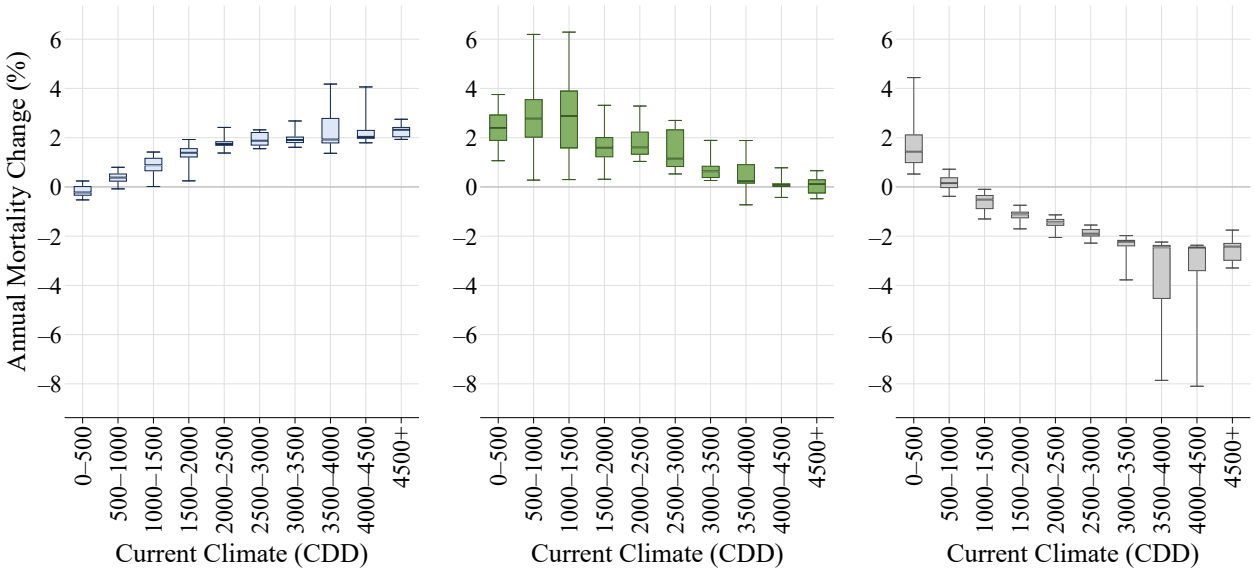

(a) Homogeneous Effects, No Adaptation

(b) Current Climate Effects, No Adaptation

(c) Current Climate Effects, Future Adaptation

Notes: The figure summarizes annual mortality effects of end-of-century (2080–2099) climate change relative to the current period (1992–2013) under the RCP 8.5 emissions scenario, as predicted by the MPI-ESM-LR model. Box and whisker plots summarize ZIP code-level effects by current climate. Additional notes in Appendix Figure B.9a.

Figure B.9s: MPI-ESM-MR: End-of-Century Climate Change Effects (RCP 8.5)

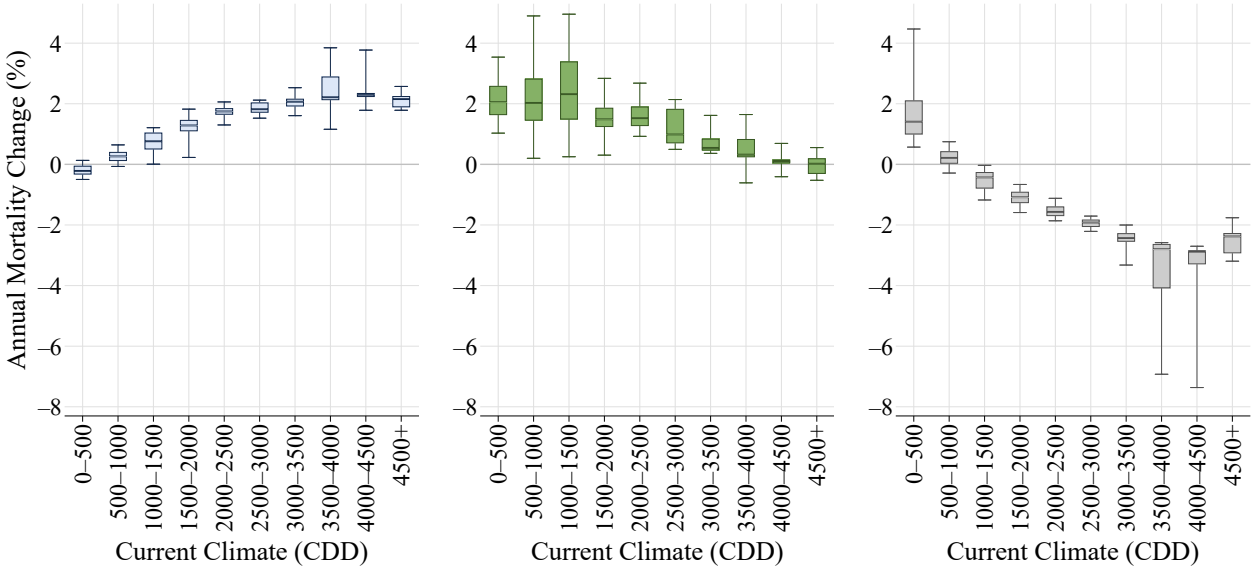

(a) Homogeneous Effects, No Adaptation

(b) Current Climate Effects, No Adaptation

(c) Current Climate Effects, Future Adaptation

Notes: The figure summarizes annual mortality effects of end-of-century (2080–2099) climate change relative to the current period (1992–2013) under the RCP 8.5 emissions scenario, as predicted by the MPI-ESM-MR model. Box and whisker plots summarize ZIP code-level effects by current climate. Additional notes in Appendix Figure B.9a.

Figure B.9t: MRI-CGCM3: End-of-Century Climate Change Effects (RCP 8.5)

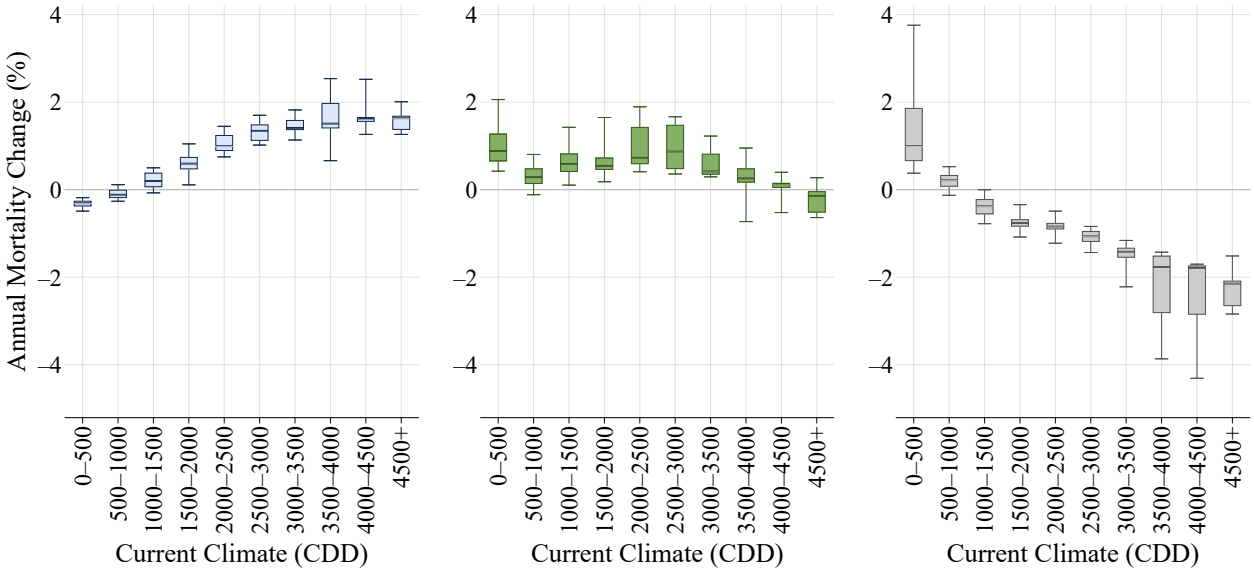

(a) Homogeneous Effects, No Adaptation

(b) Current Climate Effects, No Adaptation

(c) Current Climate Effects, Future Adaptation

Notes: The figure summarizes annual mortality effects of end-of-century (2080–2099) climate change relative to the current period (1992–2013) under the RCP 8.5 emissions scenario, as predicted by the MRI-CGCM3 model. Box and whisker plots summarize ZIP code-level effects by current climate. Additional notes in Appendix Figure B.9a.

Figure B.9u: NorESM1-M: End-of-Century Climate Change Effects (RCP 8.5)

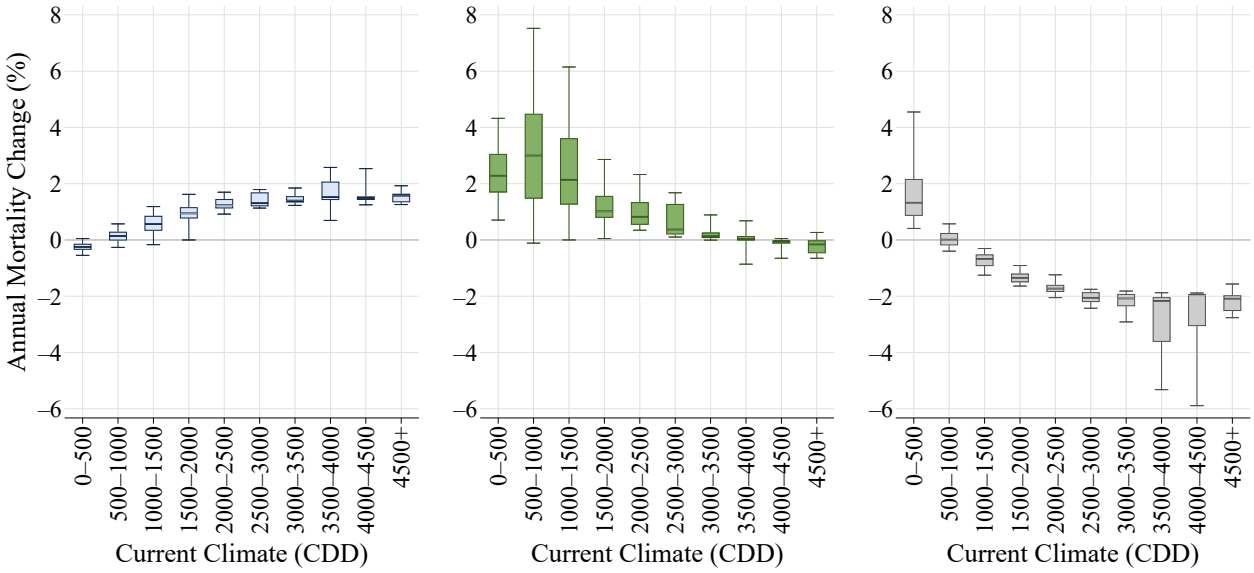

(a) Homogeneous Effects, No Adaptation

(b) Current Climate Effects, No Adaptation

(c) Current Climate Effects, Future Adaptation

Notes: The figure summarizes annual mortality effects of end-of-century (2080–2099) climate change relative to the current period (1992–2013) under the RCP 8.5 emissions scenario, as predicted by the NorESM1-M model. Box and whisker plots summarize ZIP code-level effects by current climate. Additional notes in Appendix Figure B.9a.

Figure B.9v: bcc-csm1-1: End-of-Century Climate Change Effects (RCP 8.5)

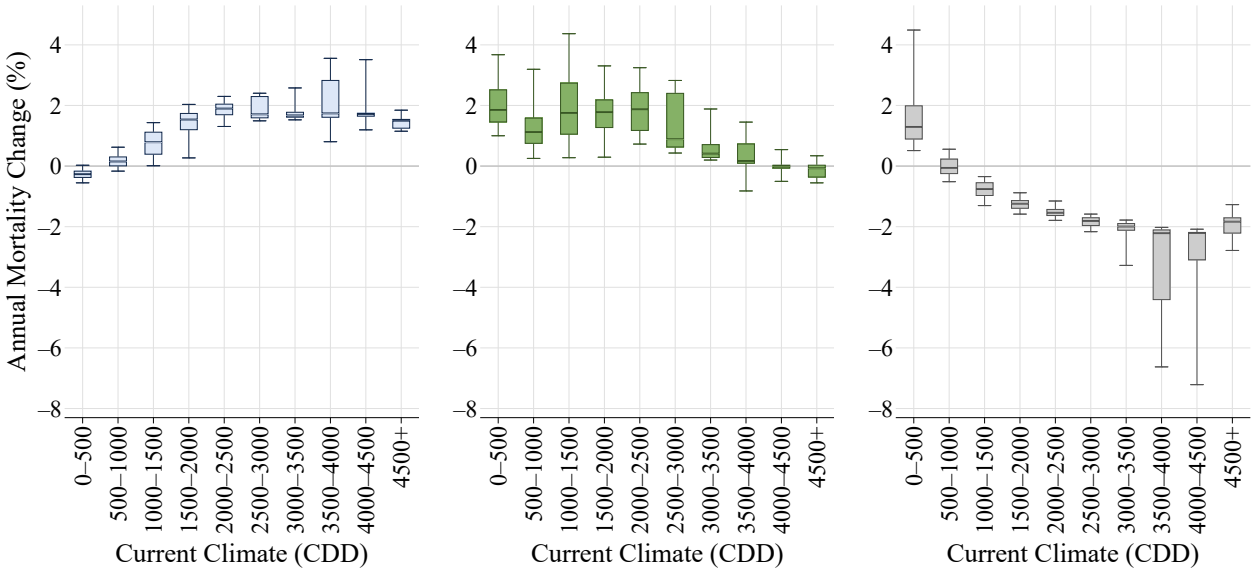

(a) Homogeneous Effects, No Adaptation

(b) Current Climate Effects, No Adaptation

(c) Current Climate Effects, Future Adaptation

Notes: The figure summarizes annual mortality effects of end-of-century (2080–2099) climate change relative to the current period (1992–2013) under the RCP 8.5 emissions scenario, as predicted by the bcc-csm1-1 model. Box and whisker plots summarize ZIP code-level effects by current climate. Additional notes in Appendix Figure B.9a.

Figure B.9w: inmcm4: End-of-Century Climate Change Effects (RCP 8.5)

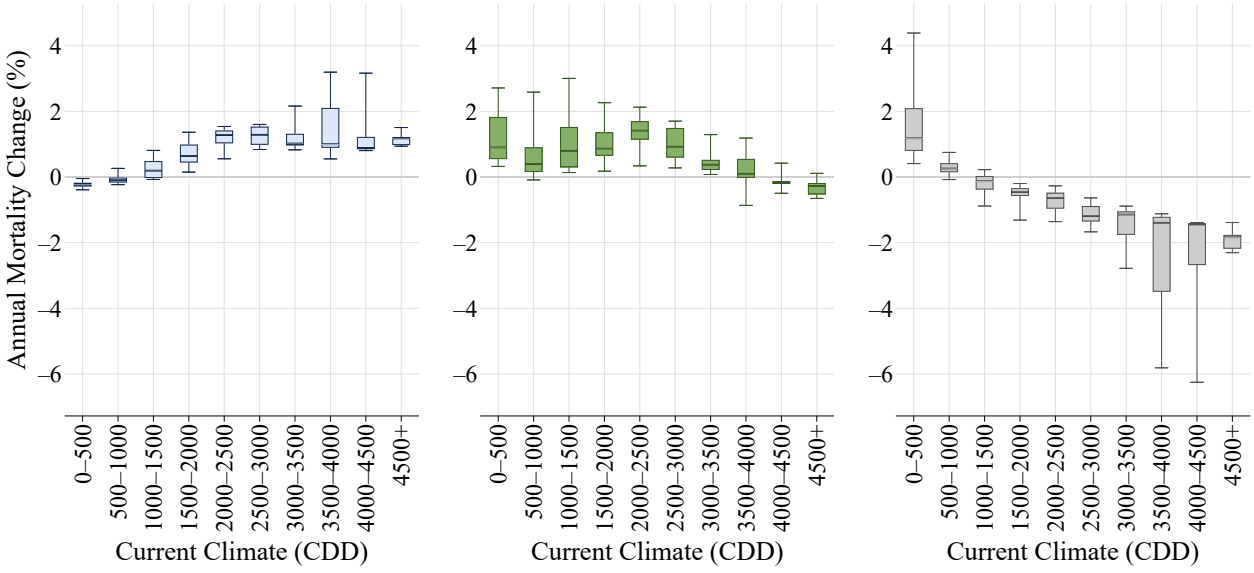

(a) Homogeneous Effects, No Adaptation

(b) Current Climate Effects, No Adaptation

(c) Current Climate Effects, Future Adaptation

Notes: The figure summarizes annual mortality effects of end-of-century (2080–2099) climate change relative to the current period (1992–2013) under the RCP 8.5 emissions scenario, as predicted by the inmcm4 model. Box and whisker plots summarize ZIP code-level effects by current climate. Additional notes in Appendix Figure B.9a.

Figure B.10: Weighted Meta Model: End-of-Century Climate Change Effects (RCP 4.5)

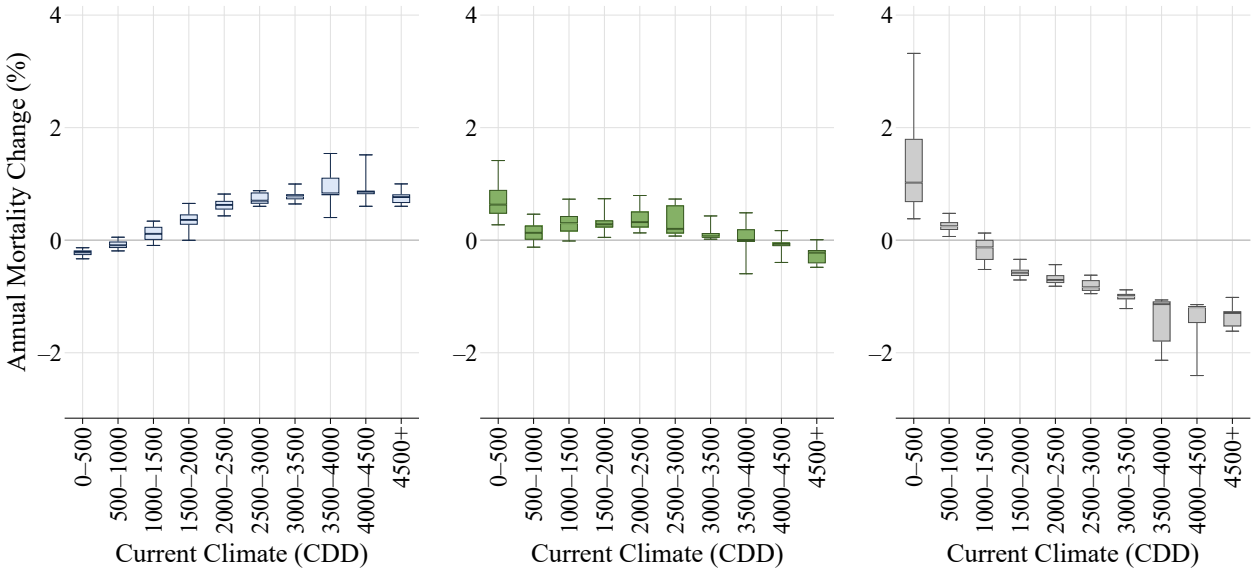

(a) Homogeneous Effects, No Adaptation

(b) Current Climate Effects, No Adaptation

(c) Current Climate Effects, Future Adaptation

Notes: The figure summarizes annual mortality effects of end-of-century (2080–2099) climate change relative to the current period (1992–2013) under the RCP 4.5 emissions scenario, as predicted by the weighted-meta-NEX-GDDP model. Observations are at the ZIP code level and are grouped by current climate (CDD). Box and whisker plots summarize the distribution of climate change effects across ZIP codes in each climate range. Boxes stretch from the 25th percentile (lower hinge) to the 75th percentile (upper hinge). The median is plotted as a line across the box. Whiskers stretch from the 5th percentile to the 95th percentile. Statistics are weighted by the elderly Medicare population in each ZIP code. Appendix Table B.4 summarizes these climate change impacts, aggregated to climate terciles and to the United States as a whole.

Figure B.11: Weighted Meta Model: End-of-Century Climate Change Effects (RCP 8.5, PRISM)

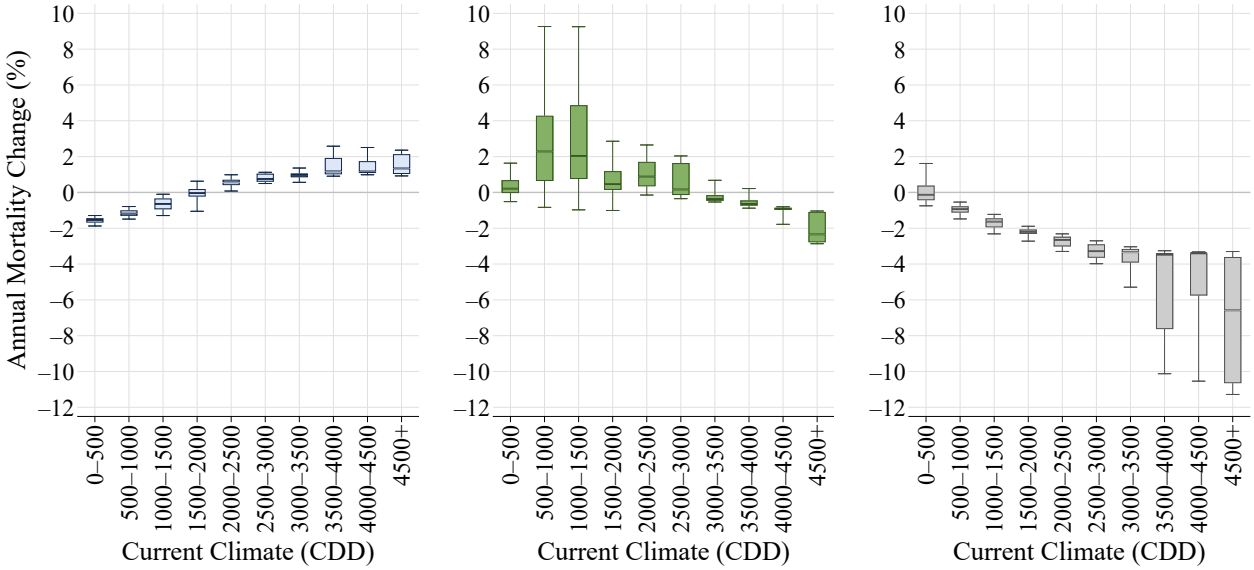

(a) Homogeneous Effects, No Adaptation

(b) Current Climate Effects, No Adaptation

(c) Current Climate Effects, Future Adaptation

Notes: The figure summarizes annual mortality effects of end-of-century (2080–2099) climate change relative to the current period (1992–2013) under the RCP 8.5 emissions scenario, as predicted by the weighted-meta-NEX-GDDP model. Observations are at the ZIP code level and are grouped by current climate (CDD). Box and whisker plots summarize the distribution of climate change effects across ZIP codes in each climate range. Boxes stretch from the 25th percentile (lower hinge) to the 75th percentile (upper hinge). The median is plotted as a line across the box. Whiskers stretch from the 5th percentile to the 95th percentile. Statistics are weighted by the elderly Medicare population in each ZIP code. Appendix Table B.3 summarizes these climate change impacts, aggregated to climate terciles and to the United States as a whole.

Figure B.12a: Differential Effects of Temperature by Air Conditioning (AC) Penetration, Primary AC Imputation

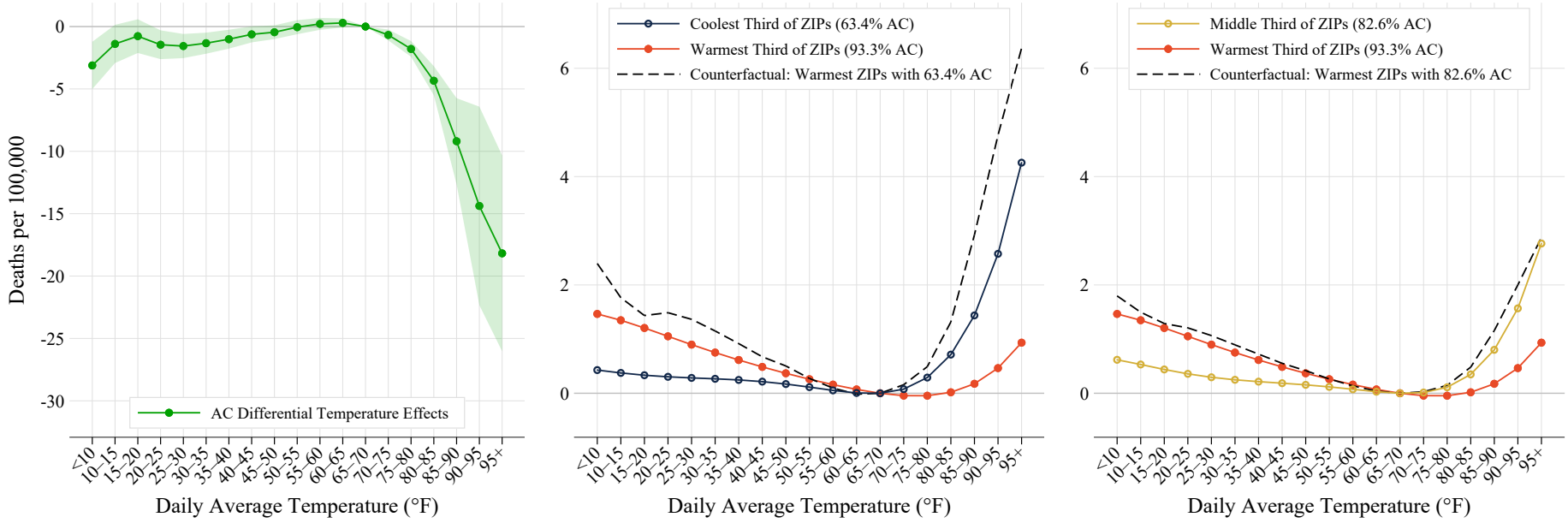

(a) Estimation (b) Counterfactual 1 (c) Counterfactual 2

Notes: Panel (a) reports estimates of how the mortality effects of temperature vary with regional AC penetration. The estimates come from estimating a version of Equation 1 where daily average temperature bins are interacted with ZIP code-level AC penetration instead of with climate tercile indicators and separate temperature controls for each Census Region are added. The shaded region reports 95 percent confidence intervals based on two-way clustered standard errors at the county and state×date levels. Panels (b) and (c) present the implied counterfactual mortality effects of temperature in the warmest third of ZIP codes if exposed to the lower AC penetration rates in the coolest and middle third of ZIP codes, respectively.

Figure B.12b: Differential Effects of Temperature by Air Conditioning (AC) Penetration, Alternate AC Imputation

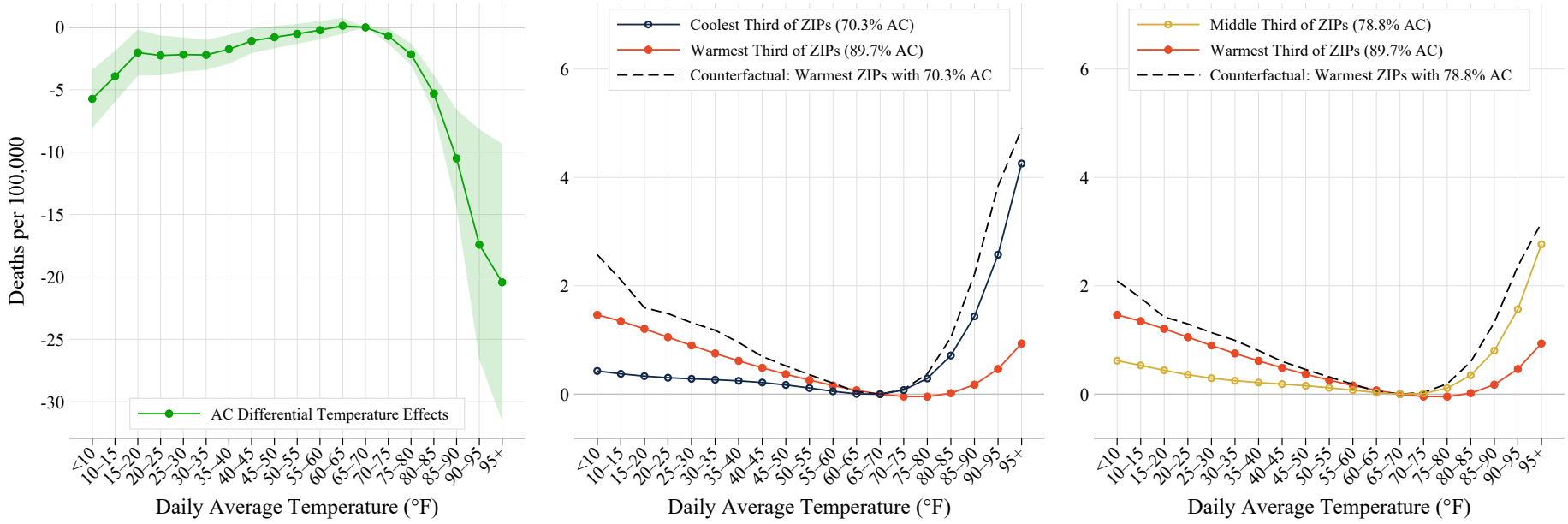

(a) Estimation (b) Counterfactual 1 (c) Counterfactual 2

Notes: This figure shows results from replicating the AC heterogeneity analysis presented in appendix figure B.12a except that the AC penetration imputation procedure described in appendix section A.4.2 was modified to exclude any climate variables. Panel (a) reports estimates of how the mortality effect of each temperature bin varies with regional AC penetration. The estimates come from estimating a version of Equation 1 where daily average temperature bins are interacted with ZIP code-level AC penetration instead of with climate tercile indicators and separate temperature controls for each Census Region are added. The shaded region reports 95 percent confidence intervals based on two-way clustered standard errors at the county and state×date levels. Panels (b) and (c) present the implied counterfactual mortality effects of temperature in the warmest third of ZIP codes if exposed to the lower AC penetration rates in the coolest and middle third of ZIP codes, respectively.

Table B.1a: Heterogeneous Effects of Temperature on Mortality (GHCN)

	(1)	(2)	(3)	(4)	(5)	(6)	(7)	(8)	(9)	(10)
			Non-parametric temperature bin estimation				Semi-parametric polynomial estimation			
	Freq. (%)	3-day mort.	Coef.	Std. Err	Std. Err	Std. Err	Coef.	Std. Err	Std. Err	Std. Err
Coolest Third of ZIPs ×										
$tavg \in [-\infty, 10)$	1.72	44.0	0.43***	0.11	0.19	0.13	0.43***	0.10	0.17	0.12
$tavg \in [10, 15)$	1.52	44.2	0.34***	0.09	0.11	0.11	0.38***	0.08	0.12	0.10
$tavg \in [15, 20)$	2.53	44.0	0.29***	0.08	0.11	0.10	0.33***	0.08	0.10	0.09
$tavg \in [20, 25)$	3.88	43.7	0.26***	0.08	0.12	0.09	0.30***	0.07	0.10	0.08
$tavg \in [25, 30)$	5.33	43.3	0.31***	0.07	0.11	0.08	0.28***	0.06	0.09	0.07
$tavg \in [30, 35)$	6.96	42.6	0.25***	0.07	0.09	0.07	0.27***	0.06	0.08	0.07
$tavg \in [35, 40)$	7.78	41.8	0.23***	0.06	0.08	0.07	0.25***	0.05	0.08	0.06
$tavg \in [40, 45)$	8.33	40.9	0.18***	0.06	0.08	0.06	0.22***	0.05	0.07	0.05
$tavg \in [45, 50)$	8.85	39.9	0.15***	0.05	0.07	0.05	0.17***	0.04	0.06	0.04
$tavg \in [50, 55)$	9.30	38.7	0.07	0.04	0.07	0.05	0.11***	0.04	0.06	0.04
$tavg \in [55, 60)$	9.83	37.3	0.02	0.04	0.06	0.05	0.05*	0.03	0.04	0.03
$tavg \in [60, 65)$	10.50	36.2	–0.02	0.03	0.03	0.03	0.01	0.02	0.02	0.02
$tavg \in [65, 70)$	10.61	35.8	0.00	0.00	0.00	0.00	0.00	0.00	0.00	0.00
$tavg \in [70, 75)$	8.11	36.1	0.10**	0.04	0.05	0.04	0.08***	0.02	0.03	0.02
$tavg \in [75, 80)$	3.87	36.4	0.20***	0.05	0.07	0.05	0.29***	0.04	0.08	0.04
$tavg \in [80, 85)$	0.81	37.0	0.68***	0.11	0.20	0.11	0.71***	0.09	0.19	0.10
$tavg \in [85, 90)$	0.06	37.7	1.80***	0.34	0.64	0.39	1.44***	0.21	0.38	0.24
$tavg \in [90, 95)$	< 0.002	48.8	11.78***	4.26	4.73	4.42	2.57***	0.43	0.72	0.49
$tavg \in [95, \infty]$	< 0.002	43.6	14.08	16.94	18.34	17.40	4.26***	0.81	1.27	0.92
Middle Third of ZIPs ×										
$tavg \in [-\infty, 10)$	0.45	46.9	0.58***	0.16	0.20	0.19	0.62***	0.15	0.21	0.19
$tavg \in [10, 15)$	0.58	46.4	0.51***	0.13	0.15	0.15	0.53***	0.10	0.13	0.12
$tavg \in [15, 20)$	1.18	45.9	0.50***	0.12	0.13	0.14	0.44***	0.08	0.10	0.10
$tavg \in [20, 25)$	2.26	45.2	0.19*	0.10	0.10	0.11	0.36***	0.08	0.09	0.09
$tavg \in [25, 30)$	3.80	44.5	0.26***	0.09	0.10	0.10	0.30***	0.08	0.09	0.09
$tavg \in [30, 35)$	5.63	43.9	0.22**	0.08	0.10	0.09	0.25***	0.08	0.10	0.08
$tavg \in [35, 40)$	7.09	43.1	0.21**	0.07	0.08	0.08	0.21***	0.08	0.10	0.08
$tavg \in [40, 45)$	7.52	42.2	0.17**	0.07	0.09	0.07	0.19**	0.07	0.10	0.07
$tavg \in [45, 50)$	7.81	41.0	0.12	0.07	0.08	0.08	0.16**	0.06	0.09	0.07
$tavg \in [50, 55)$	8.62	39.9	0.03	0.06	0.05	0.06	0.12**	0.05	0.08	0.06
$tavg \in [55, 60)$	9.40	38.9	–0.01	0.04	0.05	0.05	0.07*	0.04	0.06	0.04
$tavg \in [60, 65)$	9.78	37.7	–0.00	0.03	0.03	0.03	0.03	0.02	0.03	0.02
$tavg \in [65, 70)$	10.70	36.5	0.00	0.00	0.00	0.00	0.00	0.00	0.00	0.00
$tavg \in [70, 75)$	11.84	36.0	0.02	0.03	0.05	0.03	0.01	0.02	0.03	0.02
$tavg \in [75, 80)$	9.30	36.1	0.08	0.06	0.09	0.06	0.11**	0.05	0.06	0.05
$tavg \in [80, 85)$	3.45	36.2	0.25***	0.09	0.12	0.09	0.35***	0.10	0.11	0.10
$tavg \in [85, 90)$	0.54	36.8	0.71***	0.18	0.17	0.19	0.80***	0.22	0.21	0.23
$tavg \in [90, 95)$	0.03	39.7	3.76***	1.40	1.56	1.41	1.57***	0.45	0.41	0.46
$tavg \in [95, \infty]$	< 0.002	41.2	1.03	5.21	4.10	5.12	2.77***	0.83	0.77	0.86
Warmest Third of ZIPs ×										
$tavg \in [-\infty, 10)$	0.02	51.7	1.13	0.88	1.27	0.94	1.46**	0.66	0.91	0.71
$tavg \in [10, 15)$	0.04	50.5	1.42**	0.55	0.37	0.58	1.35***	0.36	0.49	0.39
$tavg \in [15, 20)$	0.11	50.1	1.33***	0.33	0.43	0.35	1.21***	0.19	0.26	0.22
$tavg \in [20, 25)$	0.28	49.2	1.14***	0.17	0.18	0.19	1.05***	0.12	0.15	0.14
$tavg \in [25, 30)$	0.68	48.0	0.88***	0.12	0.12	0.14	0.90***	0.08	0.11	0.10
$tavg \in [30, 35)$	1.45	47.1	0.70***	0.09	0.10	0.10	0.75***	0.07	0.10	0.08
$tavg \in [35, 40)$	2.77	46.0	0.63***	0.07	0.09	0.08	0.61***	0.06	0.09	0.07
$tavg \in [40, 45)$	4.48	45.0	0.49***	0.06	0.10	0.07	0.49***	0.05	0.08	0.06
$tavg \in [45, 50)$	6.00	43.8	0.40***	0.06	0.07	0.06	0.37***	0.05	0.07	0.05
$tavg \in [50, 55)$	7.11	42.7	0.27***	0.05	0.07	0.06	0.26***	0.04	0.06	0.04
$tavg \in [55, 60)$	8.02	41.6	0.14***	0.04	0.05	0.04	0.16***	0.03	0.04	0.03
$tavg \in [60, 65)$	8.74	40.5	0.08**	0.03	0.04	0.03	0.07***	0.01	0.02	0.01
$tavg \in [65, 70)$	10.04	39.4	0.00	0.00	0.00	0.00	0.00	0.00	0.00	0.00
$tavg \in [70, 75)$	12.63	38.0	–0.02	0.03	0.03	0.04	–0.04***	0.01	0.02	0.01
$tavg \in [75, 80)$	16.19	36.8	–0.04	0.04	0.04	0.05	–0.05	0.03	0.05	0.03
$tavg \in [80, 85)$	15.96	36.4	0.04	0.06	0.07	0.06	0.02	0.05	0.08	0.05
$tavg \in [85, 90)$	4.30	36.2	0.15*	0.08	0.11	0.08	0.18**	0.07	0.11	0.07
$tavg \in [90, 95)$	0.92	35.0	0.46***	0.10	0.10	0.10	0.46***	0.09	0.15	0.09
$tavg \in [95, \infty]$	0.25	35.0	1.06***	0.17	0.25	0.18	0.93***	0.15	0.23	0.15
Dependent variable			3-day mort.	3-day mort.	3-day mort.	3-day mort.	3-day mort.	3-day mort.	3-day mort.	3-day mort.
Dep. var. mean			39.40	39.40	39.40	39.40	39.40	39.40	39.40	39.40
Observations	250, 247, 311	250, 247, 311	250, 247, 311	250, 247, 311	250, 247, 311	250, 247, 311	250, 247, 311	250, 247, 311	250, 247, 311	250, 247, 311
First cluster level			county	county	state	county	county	county	state	county
Second cluster level			state × date			state × date	state × date			state × date
Weather source	GHCN	GHCN	GHCN	GHCN	GHCN	GHCN	GHCN	GHCN	GHCN	GHCN

Notes: This table provides sample summary statistics and estimated 3-day mortality effects of temperature as measured by GHCN data. An observation is a ZIP code day. Columns (1) and (2) summarize the sample distributions of realized temperature and 3-day mortality across each of 19 temperature bins. Columns (3)–(10) report results from estimating Equation 1. Columns (3)–(6) report non-parametric temperature bin estimates and standard errors under various levels of clustering. Columns (7)–(10) report semi-parametric (5th order polynomial in the temperature bin) estimates and associated standard errors. Figure 2a plots a selection of these estimates.

Table B.1b: Homogeneous Effects of Temperature on Mortality (GHCN)

	(1)	(2)	(3)	(4)	(5)	(6)	(7)	(8)	(9)	(10)
			Non-parametric temperature bin estimation				Semi-parametric polynomial estimation			
	Freq. (%)	3-day mort.	Coef.	Std. Err	Std. Err	Std. Err	Coef.	Std. Err	Std. Err	Std. Err
All U.S. ZIPs										
$tavg \in [-\infty, 10)$	0.73	44.6	0.65***	0.09	0.15	0.11	0.66***	0.08	0.14	0.11
$tavg \in [10, 15)$	0.72	44.9	0.57***	0.07	0.10	0.09	0.56***	0.06	0.10	0.08
$tavg \in [15, 20)$	1.28	44.8	0.54***	0.06	0.09	0.08	0.50***	0.05	0.08	0.07
$tavg \in [20, 25)$	2.14	44.5	0.41***	0.06	0.09	0.07	0.46***	0.05	0.08	0.06
$tavg \in [25, 30)$	3.27	44.1	0.45***	0.05	0.08	0.06	0.43***	0.05	0.08	0.05
$tavg \in [30, 35)$	4.68	43.6	0.39***	0.05	0.07	0.05	0.40***	0.04	0.07	0.05
$tavg \in [35, 40)$	5.88	43.0	0.36***	0.04	0.07	0.05	0.35***	0.04	0.07	0.05
$tavg \in [40, 45)$	6.77	42.2	0.30***	0.04	0.07	0.04	0.30***	0.04	0.07	0.04
$tavg \in [45, 50)$	7.55	41.3	0.24***	0.04	0.06	0.04	0.23***	0.03	0.06	0.04
$tavg \in [50, 55)$	8.34	40.3	0.14***	0.03	0.05	0.03	0.16***	0.03	0.05	0.03
$tavg \in [55, 60)$	9.08	39.1	0.06**	0.03	0.04	0.03	0.09***	0.02	0.04	0.02
$tavg \in [60, 65)$	9.67	38.0	0.03	0.02	0.03	0.02	0.03***	0.01	0.02	0.01
$tavg \in [65, 70)$	10.45	37.2	0.00	0.00	0.00	0.00	0.00	0.00	0.00	0.00
$tavg \in [70, 75)$	10.86	36.8	0.03*	0.02	0.03	0.02	0.01	0.01	0.03	0.01
$tavg \in [75, 80)$	9.79	36.5	0.07**	0.04	0.06	0.04	0.08***	0.03	0.06	0.03
$tavg \in [80, 85)$	6.75	36.4	0.23***	0.05	0.10	0.05	0.24***	0.05	0.09	0.05
$tavg \in [85, 90)$	1.64	36.3	0.44***	0.08	0.15	0.08	0.49***	0.08	0.14	0.08
$tavg \in [90, 95)$	0.32	35.2	1.02***	0.23	0.29	0.23	0.87***	0.13	0.21	0.13
$tavg \in [95, \infty]$	0.08	35.0	1.59***	0.27	0.40	0.27	1.41***	0.22	0.33	0.23
Dependent variable			3-day mort.	3-day mort.	3-day mort.	3-day mort.	3-day mort.	3-day mort.	3-day mort.	3-day mort.
Dep. var. mean			39.40	39.40	39.40	39.40	39.40	39.40	39.40	39.40
Observations	250,247,311	250,247,311	250,247,311	250,247,311	250,247,311	250,247,311	250,247,311	250,247,311	250,247,311	250,247,311
First cluster level			county	county	state	county	county	county	state	county
Second cluster level			state × date			state × date	state × date			state × date
Weather source	GHCN	GHCN	GHCN	GHCN	GHCN	GHCN	GHCN	GHCN	GHCN	GHCN

Notes: This table provides sample summary statistics and estimated 3-day mortality effects of temperature as measured by GHCN data. An observation is a ZIP code day. Columns (1) and (2) summarize the sample distributions of realized temperature and 3-day mortality across each of 19 temperature bins. Columns (3)–(10) report results from estimating Equation 1, but with temperature effects constrained to be the same across all regions. Columns (3)–(6) report non-parametric temperature bin estimates and standard errors under various levels of clustering. Columns (7)–(10) report semi-parametric (5th order polynomial in the temperature bin) estimates and associated standard errors. Figure 2b plots a selection of these estimates.

Table B.1c: Heterogeneous Effects of Temperature on Mortality (PRISM)

	(1)	(2)	(3)	(4)	(5)	(6)	(7)	(8)	(9)	(10)
			Non-parametric temperature bin estimation				Semi-parametric polynomial estimation			
	Freq. (%)	3-day mort.	Coef.	Std. Err	Std. Err	Std. Err	Coef.	Std. Err	Std. Err	Std. Err
Coolest Third of ZIPs ×										
$tavg \in [-\infty, 10)$	1.91	44.3	1.32***	0.10	0.14	0.12	1.32***	0.09	0.15	0.12
$tavg \in [10, 15)$	1.63	44.4	1.12***	0.09	0.11	0.11	1.22***	0.08	0.11	0.09
$tavg \in [15, 20)$	2.70	44.2	1.08***	0.08	0.08	0.09	1.14***	0.07	0.09	0.08
$tavg \in [20, 25)$	3.96	43.8	1.03***	0.07	0.08	0.08	1.07***	0.06	0.08	0.07
$tavg \in [25, 30)$	5.42	43.3	0.98***	0.06	0.09	0.07	1.00***	0.06	0.08	0.07
$tavg \in [30, 35)$	7.00	42.6	0.91***	0.06	0.07	0.07	0.93***	0.05	0.07	0.06
$tavg \in [35, 40)$	7.86	41.8	0.80***	0.06	0.06	0.06	0.84***	0.05	0.06	0.06
$tavg \in [40, 45)$	8.37	40.8	0.67***	0.05	0.05	0.06	0.73***	0.04	0.05	0.05
$tavg \in [45, 50)$	8.80	39.8	0.55***	0.05	0.04	0.05	0.60***	0.04	0.05	0.04
$tavg \in [50, 55)$	9.20	38.6	0.37***	0.04	0.04	0.04	0.45***	0.03	0.04	0.04
$tavg \in [55, 60)$	9.74	37.3	0.24***	0.04	0.04	0.04	0.28***	0.02	0.03	0.03
$tavg \in [60, 65)$	10.47	36.2	0.09***	0.03	0.02	0.03	0.12***	0.01	0.02	0.01
$tavg \in [65, 70)$	10.40	35.8	0.00	0.00	0.00	0.00	0.00	0.00	0.00	0.00
$tavg \in [70, 75)$	8.01	36.0	–0.07*	0.03	0.03	0.04	–0.04**	0.01	0.02	0.02
$tavg \in [75, 80)$	3.72	36.3	–0.05	0.05	0.07	0.05	0.07*	0.04	0.06	0.04
$tavg \in [80, 85)$	0.76	36.9	0.43***	0.10	0.15	0.11	0.40***	0.09	0.15	0.10
$tavg \in [85, 90)$	0.06	37.2	1.34***	0.37	0.55	0.40	1.05***	0.20	0.34	0.23
$tavg \in [90, 95)$	< 0.002	49.8	13.09***	4.04	4.48	4.66	2.16***	0.42	0.69	0.49
$tavg \in [95, \infty]$	< 0.002	109.9	31.48***	4.16	4.17	4.24	3.85***	0.80	1.25	0.92
Middle Third of ZIPs ×										
$tavg \in [-\infty, 10)$	0.53	46.9	1.77***	0.16	0.15	0.19	1.83***	0.15	0.16	0.19
$tavg \in [10, 15)$	0.67	46.6	1.73***	0.12	0.13	0.15	1.61***	0.09	0.10	0.11
$tavg \in [15, 20)$	1.32	45.8	1.39***	0.10	0.09	0.12	1.44***	0.07	0.09	0.09
$tavg \in [20, 25)$	2.41	45.2	1.20***	0.08	0.08	0.10	1.29***	0.07	0.08	0.08
$tavg \in [25, 30)$	4.00	44.5	1.15***	0.07	0.08	0.08	1.17***	0.06	0.08	0.07
$tavg \in [30, 35)$	5.78	43.9	1.04***	0.06	0.06	0.07	1.06***	0.06	0.08	0.07
$tavg \in [35, 40)$	7.15	43.0	0.96***	0.06	0.08	0.07	0.95***	0.06	0.08	0.07
$tavg \in [40, 45)$	7.49	42.1	0.85***	0.06	0.07	0.06	0.83***	0.06	0.07	0.06
$tavg \in [45, 50)$	7.88	40.9	0.63***	0.06	0.07	0.06	0.69***	0.05	0.07	0.06
$tavg \in [50, 55)$	8.61	39.9	0.47***	0.05	0.04	0.05	0.52***	0.05	0.06	0.05
$tavg \in [55, 60)$	9.22	38.9	0.28***	0.04	0.04	0.04	0.34***	0.03	0.04	0.04
$tavg \in [60, 65)$	9.71	37.6	0.14***	0.04	0.03	0.04	0.16***	0.02	0.02	0.02
$tavg \in [65, 70)$	10.61	36.5	0.00	0.00	0.00	0.00	0.00	0.00	0.00	0.00
$tavg \in [70, 75)$	11.78	36.0	–0.07**	0.03	0.02	0.03	–0.10***	0.02	0.02	0.02
$tavg \in [75, 80)$	9.07	36.0	–0.11***	0.04	0.04	0.04	–0.09***	0.03	0.03	0.03
$tavg \in [80, 85)$	3.29	36.1	–0.00	0.06	0.06	0.06	0.10	0.08	0.07	0.08
$tavg \in [85, 90)$	0.46	36.8	0.60***	0.22	0.19	0.22	0.54**	0.21	0.18	0.22
$tavg \in [90, 95)$	0.02	39.5	3.89**	1.84	2.20	1.96	1.36***	0.47	0.41	0.49
$tavg \in [95, \infty]$	< 0.002	31.7	–8.76**	5.25	4.53	4.07	2.67***	0.92	0.81	0.97
Warmest Third of ZIPs ×										
$tavg \in [-\infty, 10)$	0.03	51.5	2.40***	0.64	0.95	0.77	2.53***	0.49	0.69	0.57
$tavg \in [10, 15)$	0.05	50.5	2.00***	0.36	0.30	0.40	2.22***	0.26	0.35	0.30
$tavg \in [15, 20)$	0.14	50.0	2.16***	0.25	0.28	0.27	1.98***	0.14	0.17	0.17
$tavg \in [20, 25)$	0.35	49.1	1.84***	0.14	0.13	0.17	1.78***	0.09	0.10	0.12
$tavg \in [25, 30)$	0.80	48.0	1.55***	0.10	0.09	0.12	1.60***	0.07	0.09	0.09
$tavg \in [30, 35)$	1.69	47.1	1.39***	0.08	0.09	0.10	1.42***	0.06	0.08	0.08
$tavg \in [35, 40)$	3.13	46.0	1.20***	0.07	0.09	0.08	1.23***	0.05	0.07	0.07
$tavg \in [40, 45)$	4.89	44.9	1.02***	0.06	0.06	0.07	1.03***	0.05	0.07	0.06
$tavg \in [45, 50)$	6.49	43.8	0.84***	0.05	0.07	0.06	0.82***	0.04	0.06	0.05
$tavg \in [50, 55)$	7.52	42.6	0.56***	0.05	0.06	0.05	0.60***	0.04	0.05	0.04
$tavg \in [55, 60)$	8.28	41.6	0.38***	0.04	0.04	0.04	0.38***	0.03	0.04	0.03
$tavg \in [60, 65)$	9.08	40.5	0.13***	0.04	0.04	0.04	0.18***	0.01	0.02	0.01
$tavg \in [65, 70)$	10.20	39.4	0.00	0.00	0.00	0.00	0.00	0.00	0.00	0.00
$tavg \in [70, 75)$	11.96	38.3	–0.14***	0.03	0.05	0.04	–0.14***	0.01	0.02	0.01
$tavg \in [75, 80)$	14.65	37.4	–0.22***	0.04	0.06	0.04	–0.22***	0.03	0.05	0.03
$tavg \in [80, 85)$	15.82	36.5	–0.26***	0.05	0.06	0.05	–0.23***	0.04	0.07	0.04
$tavg \in [85, 90)$	3.93	36.3	–0.15**	0.07	0.10	0.07	–0.15**	0.06	0.08	0.06
$tavg \in [90, 95)$	0.80	35.1	0.09	0.12	0.14	0.12	0.02	0.10	0.12	0.11
$tavg \in [95, \infty]$	0.19	35.5	0.25	0.23	0.24	0.23	0.31	0.21	0.23	0.21
Dependent variable			3-day mort.	3-day mort.	3-day mort.	3-day mort.	3-day mort.	3-day mort.	3-day mort.	3-day mort.
Dep. var. mean			39.54	39.54	39.54	39.54	39.54	39.54	39.54	39.54
Observations	259,433,198	259,433,198	259,433,198	259,433,198	259,433,198	259,433,198	259,433,198	259,433,198	259,433,198	259,433,198
First cluster level			county	county	state	county	county	county	state	county
Second cluster level			state × date			state × date	state × date			state × date
Weather source	PRISM	PRISM	prism	prism	prism	prism	prism	prism	prism	prism

Notes: This table provides sample summary statistics and estimated 3-day mortality effects of temperature as measured by PRISM data. An observation is a ZIP code day. Columns (1) and (2) summarize the sample distributions of realized temperature and 3-day mortality across each of 19 temperature bins. Columns (3)–(10) report results from estimating Equation 1. Columns (3)–(6) report non-parametric temperature bin estimates and standard errors under various levels of clustering. Columns (7)–(10) report semi-parametric (5th order polynomial in the temperature bin) estimates and associated standard errors. Figure B.5a plots a selection of these estimates.

Table B.1d: Homogeneous Effects of Temperature on Mortality (PRISM)

	(1)	(2)	(3)	(4)	(5)	(6)	(7)	(8)	(9)	(10)
			Non-parametric temperature bin estimation				Semi-parametric polynomial estimation			
	Freq. (%)	3-day mort.	Coef.	Std. Err	Std. Err	Std. Err	Coef.	Std. Err	Std. Err	Std. Err
All U.S. ZIPs										
$tavg \in [-\infty, 10)$	0.83	44.9	1.65***	0.08	0.12	0.10	1.67***	0.07	0.12	0.10
$tavg \in [10, 15)$	0.79	45.1	1.49***	0.07	0.09	0.09	1.49***	0.05	0.08	0.07
$tavg \in [15, 20)$	1.40	44.9	1.38***	0.05	0.07	0.07	1.38***	0.04	0.06	0.06
$tavg \in [20, 25)$	2.25	44.6	1.27***	0.05	0.06	0.06	1.29***	0.04	0.06	0.05
$tavg \in [25, 30)$	3.43	44.1	1.21***	0.04	0.06	0.05	1.21***	0.04	0.06	0.05
$tavg \in [30, 35)$	4.85	43.7	1.11***	0.04	0.06	0.05	1.12***	0.04	0.06	0.04
$tavg \in [35, 40)$	6.07	43.0	0.99***	0.04	0.06	0.04	1.00***	0.03	0.06	0.04
$tavg \in [40, 45)$	6.93	42.3	0.86***	0.03	0.05	0.04	0.86***	0.03	0.05	0.04
$tavg \in [45, 50)$	7.73	41.3	0.69***	0.03	0.05	0.04	0.69***	0.03	0.04	0.03
$tavg \in [50, 55)$	8.45	40.2	0.49***	0.03	0.03	0.03	0.51***	0.02	0.04	0.03
$tavg \in [55, 60)$	9.08	39.1	0.31***	0.02	0.03	0.03	0.32***	0.02	0.03	0.02
$tavg \in [60, 65)$	9.76	38.0	0.12***	0.02	0.02	0.02	0.14***	0.01	0.02	0.01
$tavg \in [65, 70)$	10.40	37.2	0.00	0.00	0.00	0.00	0.00	0.00	0.00	0.00
$tavg \in [70, 75)$	10.57	36.9	–0.09***	0.02	0.02	0.02	–0.09***	0.01	0.02	0.01
$tavg \in [75, 80)$	9.11	36.8	–0.13***	0.03	0.04	0.03	–0.11***	0.02	0.04	0.02
$tavg \in [80, 85)$	6.56	36.5	–0.07*	0.04	0.06	0.04	–0.04	0.04	0.07	0.04
$tavg \in [85, 90)$	1.46	36.3	0.18**	0.08	0.14	0.09	0.16*	0.08	0.12	0.08
$tavg \in [90, 95)$	0.27	35.3	0.66**	0.26	0.33	0.27	0.49***	0.16	0.22	0.17
$tavg \in [95, \infty]$	0.06	35.5	0.79**	0.33	0.39	0.34	0.98***	0.31	0.40	0.32
Dependent variable			3-day mort.	3-day mort.	3-day mort.	3-day mort.	3-day mort.	3-day mort.	3-day mort.	3-day mort.
Dep. var. mean			39.54	39.54	39.54	39.54	39.54	39.54	39.54	39.54
Observations	259,433,198	259,433,198	259,433,198	259,433,198	259,433,198	259,433,198	259,433,198	259,433,198	259,433,198	259,433,198
First cluster level			county	county	state	county	county	county	state	county
Second cluster level			state × date			state × date	state × date			state × date
Weather source	PRISM	PRISM	prism	prism	prism	prism	prism	prism	prism	prism

Notes: This table provides sample summary statistics and estimated 3-day mortality effects of temperature as measured by PRISM data. An observation is a ZIP code day. Columns (1) and (2) summarize the sample distributions of realized temperature and 3-day mortality across each of 19 temperature bins. Columns (3)–(10) report results from estimating Equation 1, but with temperature effects constrained to be the same across all regions. Columns (3)–(6) report non-parametric temperature bin estimates and standard errors under various levels of clustering. Columns (7)–(10) report semi-parametric (5th order polynomial in the temperature bin) estimates and associated standard errors. Figure B.5b plots a selection of these estimates.

Table B.2a: End-of-Century Climate Change Effects (RCP 8.5): All U.S. ZIPs

	(1)	(2)	(3)	(4)	(5)	(6)	(7)	(8)
						Annual Mortality Change (%)		
		Avg. Temp. (°F)		Annual CDD		Homogeneous Effects	Climate Heterogeneity	
	Model Weight	Current	Future	Current	Future	No Adaptation	No Adaptation	Future Adaptation
Average of NEX-GDDP Models								
Meta-model, weighted average		57.1	65.1	1413	2864	0.76***	2.15***	-0.53*
						(0.18)	(0.47)	(0.32)
Meta-model, unweighted average		57.1	65.3	1413	2897	0.79***	2.12***	-0.57*
						(0.18)	(0.45)	(0.33)
NEX-GDDP Models								
ACCESS1-0	1.02	57.1	66.7	1413	3215	1.12***	4.47***	-0.74*
						(0.23)	(1.24)	(0.45)
BNU-ESM	0.68	57.1	66.2	1413	2979	0.69***	1.62***	-0.76**
						(0.18)	(0.27)	(0.35)
CCSM4	0.68	57.1	64.1	1413	2707	0.59***	1.34***	-0.38
						(0.15)	(0.25)	(0.28)
CESM1-BGC	0.64	57.1	64.4	1413	2681	0.55***	1.25***	-0.44
						(0.14)	(0.24)	(0.27)
CNRM-CM5	1.01	57.1	64.4	1413	2613	0.46***	0.92***	-0.45*
						(0.14)	(0.17)	(0.25)
CSIRO-Mk3-6-0	0.74	57.1	65.5	1413	2941	0.83***	2.01***	-0.65*
						(0.19)	(0.37)	(0.34)
CanESM2	0.63	57.1	66.1	1413	3193	1.00***	2.30***	-0.88**
						(0.21)	(0.37)	(0.44)
GFDL-CM3	0.95	57.1	67.1	1413	3413	1.40***	4.44***	-1.07**
						(0.27)	(1.05)	(0.53)
GFDL-ESM2G	0.44	57.1	63.7	1413	2599	0.54***	0.87***	-0.43
						(0.14)	(0.14)	(0.26)
GFDL-ESM2M	0.43	57.1	63.0	1413	2497	0.50***	0.69***	-0.37
						(0.12)	(0.12)	(0.24)
IPSL-CM5A-LR	0.72	57.1	66.3	1413	3099	1.00***	3.18***	-0.81**
						(0.22)	(0.75)	(0.39)
IPSL-CM5A-MR	0.82	57.1	66.2	1413	3174	1.21***	4.86***	-0.70*
						(0.24)	(1.38)	(0.41)
MIROC-ESM	0.15	57.1	67.7	1413	3370	1.20***	3.14***	-1.28**
						(0.26)	(0.58)	(0.52)
MIROC-ESM-CHEM	0.17	57.1	68.5	1413	3464	1.21***	2.91***	-1.57***
						(0.27)	(0.50)	(0.55)
MIROC5	1.11	57.1	65.7	1413	2839	0.58***	1.13***	-0.78**
						(0.17)	(0.20)	(0.32)
MPI-ESM-LR	0.49	57.1	64.9	1413	2925	0.88***	2.32***	-0.49
						(0.18)	(0.49)	(0.35)
MPI-ESM-MR	0.52	57.1	64.6	1413	2845	0.80***	1.93***	-0.46
						(0.17)	(0.38)	(0.33)
MRI-CGCM3	0.68	57.1	62.7	1413	2344	0.34***	0.58***	-0.24
						(0.10)	(0.11)	(0.19)
NorESM1-M	0.88	57.1	65.5	1413	2795	0.56***	2.21***	-0.55*
						(0.16)	(0.63)	(0.29)
bcc-csm1-1	0.55	57.1	65.2	1413	2881	0.75***	1.54***	-0.58*
						(0.17)	(0.24)	(0.33)
inmcm4	1.08	57.1	62.3	1413	2255	0.35***	0.88***	-0.13
						(0.10)	(0.18)	(0.16)

Notes: The table summarizes ZIP code-level climate change impacts, aggregated to the United States as a whole, under all 21 NEX-GDDP climate models and two meta-models. The climate model is given by the row label. The results for the weighted meta-model—the first listed in the table—are the same as those reported for "All U.S. ZIPs" in Table 1.

Table B.2b: End-of-Century Climate Change Effects (RCP 8.5): Coolest Third of ZIPs

	(1)	(2)	(3)	(4)	(5)	(6)	(7)	(8)
						Annual Mortality Change (%)		
		Avg. Temp. (°F)		Annual CDD		Homogeneous Effects	Climate Heterogeneity	
	Model Weight	Current	Future	Current	Future	No Adaptation	No Adaptation	Future Adaptation
Average of NEX-GDDP Models								
Meta-model, weighted average		49.4	58.1	525	1661	-0.03	2.25***	0.84**
						(0.12)	(0.50)	(0.35)
Meta-model, unweighted average		49.4	58.2	525	1683	-0.03	2.18***	0.82**
						(0.12)	(0.45)	(0.35)
NEX-GDDP Models								
ACCESS1-0	1.02	49.4	59.9	525	1979	0.17	4.65***	0.74**
						(0.16)	(1.37)	(0.36)
BNU-ESM	0.68	49.4	59.7	525	1869	-0.05	2.15***	0.61*
						(0.14)	(0.34)	(0.34)
CCSM4	0.68	49.4	57.0	525	1563	-0.03	1.64***	0.90**
						(0.10)	(0.30)	(0.36)
CESM1-BGC	0.64	49.4	57.3	525	1513	-0.08	1.52***	0.82**
						(0.10)	(0.29)	(0.35)
CNRM-CM5	1.01	49.4	57.4	525	1466	-0.16	1.14***	0.77**
						(0.10)	(0.19)	(0.36)
CSIRO-Mk3-6-0	0.74	49.4	58.6	525	1772	-0.02	2.15***	0.72**
						(0.13)	(0.39)	(0.35)
CanESM2	0.63	49.4	59.3	525	2036	0.15	2.74***	0.68*
						(0.15)	(0.46)	(0.37)
GFDL-CM3	0.95	49.4	60.0	525	2136	0.30*	4.32***	0.70*
						(0.17)	(1.02)	(0.38)
GFDL-ESM2G	0.44	49.4	56.4	525	1342	-0.19**	0.77***	0.77**
						(0.09)	(0.14)	(0.35)
GFDL-ESM2M	0.43	49.4	55.2	525	1226	-0.16**	0.63***	0.79**
						(0.07)	(0.11)	(0.33)
IPSL-CM5A-LR	0.72	49.4	59.3	525	1836	-0.02	3.03***	0.74**
						(0.13)	(0.74)	(0.35)
IPSL-CM5A-MR	0.82	49.4	58.8	525	1878	0.17	4.87***	0.95***
						(0.14)	(1.57)	(0.36)
MIROC-ESM	0.15	49.4	61.0	525	2057	-0.03	2.53***	0.41
						(0.16)	(0.41)	(0.35)
MIROC-ESM-CHEM	0.17	49.4	61.8	525	2107	-0.08	2.48***	0.26
						(0.17)	(0.40)	(0.34)
MIROC5	1.11	49.4	58.7	525	1584	-0.25**	1.07***	0.58*
						(0.11)	(0.20)	(0.33)
MPI-ESM-LR	0.49	49.4	57.8	525	1736	0.10	2.45***	0.88**
						(0.12)	(0.49)	(0.35)
MPI-ESM-MR	0.52	49.4	57.3	525	1622	0.03	1.98***	0.90**
						(0.11)	(0.36)	(0.36)
MRI-CGCM3	0.68	49.4	55.6	525	1198	-0.22***	0.55***	0.71**
						(0.07)	(0.11)	(0.33)
NorESM1-M	0.88	49.4	58.6	525	1661	-0.06	2.75***	0.77**
						(0.12)	(0.78)	(0.34)
bcc-csm1-1	0.55	49.4	58.0	525	1662	-0.07	1.47***	0.73**
						(0.12)	(0.22)	(0.34)
inmcm4	1.08	49.4	54.8	525	1105	-0.16**	0.81***	0.83***
						(0.06)	(0.18)	(0.28)

Notes: The table summarizes ZIP code-level climate change impacts, aggregated to the coolest U.S. climate tercile, under all 21 NEX-GDDP climate models and two meta-models. The climate model is given by the row label. The results for the weighted meta-model—the first listed in the table—are the same as those reported for "Coolest third of ZIPs" in Table 1.

Table B.2c: End-of-Century Climate Change Effects (RCP 8.5): Middle Third of ZIPs

	(1)	(2)	(3)	(4)	(5)	(6)	(7)	(8)
						Annual Mortality Change (%)		
		Avg. Temp. (°F)		Annual CDD		Homogeneous Effects	Climate Heterogeneity	
	Model Weight	Current	Future	Current	Future	No Adaptation	No Adaptation	Future Adaptation
Average of NEX-GDDP Models								
Meta-model, weighted average		55.2	63.5	1079	2491	0.54***	2.89***	-0.41
						(0.16)	(0.93)	(0.35)
Meta-model, unweighted average		55.2	63.6	1079	2519	0.55***	2.82***	-0.45
						(0.16)	(0.89)	(0.36)
NEX-GDDP Models								
ACCESS1-0	1.02	55.2	65.1	1079	2887	0.98***	6.85***	-0.57
						(0.22)	(2.40)	(0.49)
BNU-ESM	0.68	55.2	64.6	1079	2591	0.49***	1.83***	-0.71*
						(0.17)	(0.51)	(0.37)
CCSM4	0.68	55.2	62.5	1079	2376	0.46***	1.66***	-0.35
						(0.14)	(0.46)	(0.33)
CESM1-BGC	0.64	55.2	62.7	1079	2337	0.39***	1.52***	-0.41
						(0.13)	(0.44)	(0.31)
CNRM-CM5	1.01	55.2	62.7	1079	2231	0.26**	1.05***	-0.42
						(0.12)	(0.32)	(0.26)
CSIRO-Mk3-6-0	0.74	55.2	63.8	1079	2544	0.55***	2.44***	-0.55
						(0.16)	(0.73)	(0.36)
CanESM2	0.63	55.2	64.4	1079	2825	0.77***	2.66***	-0.75
						(0.19)	(0.70)	(0.48)
GFDL-CM3	0.95	55.2	65.4	1079	3008	1.10***	6.52***	-0.61
						(0.24)	(2.18)	(0.53)
GFDL-ESM2G	0.44	55.2	61.9	1079	2202	0.27**	0.87***	-0.33
						(0.11)	(0.25)	(0.27)
GFDL-ESM2M	0.43	55.2	61.1	1079	2069	0.22**	0.63***	-0.21
						(0.10)	(0.19)	(0.23)
IPSL-CM5A-LR	0.72	55.2	64.7	1079	2708	0.67***	4.37***	-0.60
						(0.18)	(1.51)	(0.40)
IPSL-CM5A-MR	0.82	55.2	64.4	1079	2802	0.96***	7.19***	-0.37
						(0.21)	(2.59)	(0.45)
MIROC-ESM	0.15	55.2	65.9	1079	2948	0.84***	4.25***	-0.93*
						(0.22)	(1.28)	(0.51)
MIROC-ESM-CHEM	0.17	55.2	66.8	1079	3035	0.79***	3.61***	-1.18**
						(0.23)	(1.05)	(0.51)
MIROC5	1.11	55.2	64.1	1079	2444	0.25*	1.07***	-0.71**
						(0.14)	(0.34)	(0.34)
MPI-ESM-LR	0.49	55.2	63.2	1079	2588	0.72***	3.27***	-0.38
						(0.17)	(1.00)	(0.40)
MPI-ESM-MR	0.52	55.2	62.8	1079	2456	0.60***	2.68***	-0.30
						(0.15)	(0.81)	(0.36)
MRI-CGCM3	0.68	55.2	61.0	1079	1967	0.12	0.56***	-0.19
						(0.09)	(0.20)	(0.20)
NorESM1-M	0.88	55.2	64.0	1079	2455	0.44***	3.19***	-0.49
						(0.16)	(1.14)	(0.34)
bcc-csm1-1	0.55	55.2	63.7	1079	2563	0.58***	1.90***	-0.56
						(0.16)	(0.49)	(0.38)
inmcm4	1.08	55.2	60.5	1079	1870	0.15*	1.03***	-0.03
						(0.08)	(0.36)	(0.17)

Notes: The table summarizes ZIP code-level climate change impacts, aggregated to the middle U.S. climate tercile, under all 21 NEX-GDDP climate models and two meta-models. The climate model is given by the row label. The results for the weighted meta-model—the first listed in the table—are the same as those reported for "Middle third of ZIPs" in Table 1.

Table B.2d: End-of-Century Climate Change Effects (RCP 8.5): Warmest Third of ZIPs

	(1)	(2)	(3)	(4)	(5)	(6)	(7)	(8)
						Annual Mortality Change (%)		
		Avg. Temp. (°F)		Annual CDD		Homogeneous Effects	Climate Heterogeneity	
	Model Weight	Current	Future	Current	Future	No Adaptation	No Adaptation	Future Adaptation
Average of NEX-GDDP Models								
Meta-model, weighted average		66.5	73.6	2600	4397	1.75***	1.33***	-1.97***
						(0.28)	(0.31)	(0.67)
Meta-model, unweighted average		66.5	73.8	2600	4443	1.81***	1.40***	-2.04***
						(0.29)	(0.32)	(0.69)
NEX-GDDP Models								
ACCESS1-0	1.02	66.5	74.7	2600	4736	2.18***	1.99***	-2.35***
						(0.34)	(0.45)	(0.84)
BNU-ESM	0.68	66.5	74.0	2600	4435	1.60***	0.91***	-2.14***
						(0.26)	(0.25)	(0.69)
CCSM4	0.68	66.5	72.7	2600	4143	1.32***	0.73***	-1.64***
						(0.22)	(0.19)	(0.56)
CESM1-BGC	0.64	66.5	73.0	2600	4152	1.31***	0.72***	-1.69***
						(0.22)	(0.20)	(0.57)
CNRM-CM5	1.01	66.5	72.9	2600	4102	1.25***	0.60***	-1.68***
						(0.21)	(0.19)	(0.55)
CSIRO-Mk3-6-0	0.74	66.5	73.8	2600	4463	1.93***	1.45***	-2.06***
						(0.31)	(0.32)	(0.73)
CanESM2	0.63	66.5	74.4	2600	4677	2.06***	1.52***	-2.52***
						(0.33)	(0.33)	(0.81)
GFDL-CM3	0.95	66.5	75.6	2600	5048	2.77***	2.52***	-3.24***
						(0.44)	(0.54)	(1.04)
GFDL-ESM2G	0.44	66.5	72.7	2600	4208	1.51***	0.97***	-1.69***
						(0.24)	(0.22)	(0.60)
GFDL-ESM2M	0.43	66.5	72.4	2600	4149	1.40***	0.80***	-1.67***
						(0.22)	(0.20)	(0.58)
IPSL-CM5A-LR	0.72	66.5	74.9	2600	4708	2.31***	2.18***	-2.53***
						(0.38)	(0.48)	(0.83)
IPSL-CM5A-MR	0.82	66.5	75.0	2600	4794	2.48***	2.59***	-2.62***
						(0.40)	(0.58)	(0.87)
MIROC-ESM	0.15	66.5	75.9	2600	5058	2.74***	2.65***	-3.25***
						(0.44)	(0.58)	(1.04)
MIROC-ESM-CHEM	0.17	66.5	76.6	2600	5200	2.86***	2.64***	-3.72***
						(0.46)	(0.58)	(1.13)
MIROC5	1.11	66.5	74.0	2600	4445	1.72***	1.25***	-2.16***
						(0.28)	(0.30)	(0.70)
MPI-ESM-LR	0.49	66.5	73.4	2600	4407	1.77***	1.27***	-1.94***
						(0.28)	(0.28)	(0.69)
MPI-ESM-MR	0.52	66.5	73.4	2600	4413	1.74***	1.15***	-1.95***
						(0.27)	(0.26)	(0.70)
MRI-CGCM3	0.68	66.5	71.4	2600	3823	1.09***	0.62***	-1.22***
						(0.18)	(0.16)	(0.44)
NorESM1-M	0.88	66.5	73.6	2600	4227	1.27***	0.73***	-1.90***
						(0.22)	(0.22)	(0.58)
bcc-csm1-1	0.55	66.5	73.6	2600	4376	1.71***	1.25***	-1.86***
						(0.27)	(0.28)	(0.66)
inmcm4	1.08	66.5	71.3	2600	3746	1.05***	0.79***	-1.15***
						(0.18)	(0.20)	(0.38)

Notes: The table summarizes ZIP code-level climate change impacts, aggregated to the warmest U.S. climate tercile, under all 21 NEX-GDDP climate models and two meta-models. The climate model is given by the row label. The results for the weighted meta-model—the first listed in the table—are the same as those reported for "Warmest third of ZIPs" in Table 1.

Table B.3: End-of-Century Climate Change Effects (RCP 8.5, PRISM)

	(1)	(2)	(3)	(4)	(5)	(6)	(7)
					Annual Mortality Change (%)		
	Avg. Temp. (°F)		Annual CDD		Homogeneous Effects	Climate Heterogeneity	
	Current	Future	Current	Future	No Adaptation	No Adaptation	Future Adaptation
Coolest third of ZIPs	49.5	58.1	526	1666	-1.38***	1.32**	-0.48
					(0.09)	(0.64)	(0.36)
Middle third of ZIPs	55.2	63.5	1079	2491	-0.80***	3.80**	-1.47***
					(0.15)	(1.80)	(0.32)
Warmest third of ZIPs	66.0	73.3	2526	4323	0.54	0.38	-3.13***
					(0.34)	(0.36)	(0.67)
All U.S. ZIPs	56.9	64.9	1372	2820	-0.55***	1.84**	-1.69***
					(0.18)	(0.79)	(0.30)

Notes: The table summarizes ZIP code-level climate change impacts, aggregated to climate terciles and to the United States as a whole. The table is the same as Table 1, except that the current distributions of temperature and estimated temperature-mortality relationships for ZIP codes are based off PRISM data, rather than GHCN data. Columns (1)–(4) summarize the current climate of each region as well as the end-of-century (2080–2099) climate projected by the meta-model under the RCP 8.5 greenhouse gas emissions scenario. Columns (5)–(7) are based on the ZIP code-level annual mortality effects summarized in Appendix Figure B.11. Column (5) reports climate effects under the assumption of homogeneous temperature effects. Column (6) reports "business as usual" climate effects that allow for heterogeneous temperature effects based on current climate but do not allow for future adaptation. Column (7) reports climate effects that incorporate both current heterogeneity and future adaptation.

Table B.4: End-of-Century Climate Change Effects (RCP 4.5, GHCN)

	(1)	(2)	(3)	(4)	(5)	(6)	(7)
					Annual Mortality Change (%)		
	Avg. Temp. (°F)		Annual CDD		Homogeneous Effects	Climate Heterogeneity	
	Current	Future	Current	Future	No Adaptation	No Adaptation	Future Adaptation
Coolest third of ZIPs	49.4	53.9	525	1007	-0.16***	0.36***	0.68***
					(0.05)	(0.08)	(0.26)
Middle third of ZIPs	55.2	59.4	1079	1708	0.06	0.25**	0.01
					(0.06)	(0.11)	(0.16)
Warmest third of ZIPs	66.5	70.0	2600	3429	0.62***	0.23**	-0.85***
					(0.11)	(0.09)	(0.28)
All U.S. ZIPs	57.1	61.2	1413	2061	0.18**	0.28***	-0.06
					(0.07)	(0.06)	(0.13)

Notes: The table summarizes ZIP code-level climate change impacts, aggregated to climate terciles and to the United States as a whole. Columns (1)–(4) summarize the current climate of each region as well as the end-of-century (2080–2099) climate projected by the meta-model under the RCP 4.5 greenhouse gas emissions scenario. Columns (5)–(7) are based on the ZIP code-level annual mortality effects summarized in Appendix Figure B.10. Column (5) reports climate effects under the assumption of homogeneous temperature effects. Column (6) reports "business as usual" climate effects that allow for heterogeneous temperature effects based on current climate but do not allow for future adaptation. Column (7) reports climate effects that incorporate both current heterogeneity and future adaptation.